Estuarine, Coastal and Shelf Science 146 (2014) 111–127

Contents lists available at ScienceDirect

Estuarine, Coastal and Shelf Science

journal homepage: www.elsevier.com/locate/ecss

Influence of variable water depth and turbidity on microalgae production in a shallow estuarine lake system — A modelling study

Katrin Tirok*, Ursula M. Scharler

School of Life Sciences, University of KwaZulu-Natal, Durban 4041, South Africa

ARTICLE INFO

Article history:
Received 19 December 2013
Accepted 20 May 2014
Available online 2 June 2014

Keywords:
light limitation
primary production
mathematical model
environmental variability
St. Lucia
South Africa

ABSTRACT

Strongly varying water levels and turbidities are typical characteristics of the large shallow estuarine lake system of St. Lucia, one of the largest on the African continent. This theoretical study investigated the combined effects of variable water depth and turbidity on seasonal pelagic and benthic microalgae production using a mathematical model, in order to ascertain productivity levels during variable and extreme conditions. Simulated pelagic and benthic net production varied between 0.3 and 180 g C m^{-2} $year^{-1}$ and 0 and 220 g C m^{-2} $year^{-1}$, respectively, dependent on depth, turbidity, and variability in turbidity. Although not surprising production and biomass decreased with increasing turbidity and depth. A high variability in turbidity, i.e. an alteration of calm and windy days, could reduce or enhance the seasonal pelagic and benthic production by more than 30% compared to a low variability. The day-to-day variability in wind-induced turbidity therefore influences production in the long term. On the other hand, varying water depth within a year did not significantly influence the seasonal production for turbidities representative of Lake St. Lucia. Reduced lake area and volume as observed during dry periods in Lake St. Lucia did not reduce primary production of the entire system since desiccation resulted in lower water depth and thus increased light availability. This agrees with field observations suggesting little light limitation and high areal microalgal biomass during a period with below average rainfall (2005–2011). Thus, microalgae potentially fulfil their function in the lake food-web even under extreme drought conditions. We believe that these results are of general interest to shallow aquatic ecosystems that are sensitive to drought periods due to either human or natural causes.

1. Introduction

Microalgae productivity contributes significantly to the total production of aquatic systems (MacIntyre and Cullen, 1996; Adams and Bate, 1999). Microalgae, both in the water column and in the sediment (benthos) are important primary producers and provide the nutritional basis for pelagic and benthic invertebrates and higher organisms (fish, birds). In estuarine systems, microalgae productivity is often limited by low light availability due to high turbidity originating from high suspended sediment concentrations (Cloern, 1987; Scheffer, 1998). Reasons for such high sediment concentrations in estuaries and shallow lakes are sediment transport from catchment areas, tidal activities and wind induced sediment resuspension (Winter, 1999; Dyer, 2000). The effect of turbidity on microalgae productivity is closely related to the mixing depth in stratified systems or to the total water depth in non stratified systems (Cloern, 1987). A low water depth or a low ratio of mixing to total depth generally increases the average underwater light availability reducing the negative effect of a high turbidity for primary production.

Estuaries being influenced by ocean tides as well as river run-offs are generally highly dynamic systems experiencing a high variability in their environmental parameters including salinity, temperature, depth and turbidity (e. g. Potter et al., 2010). Estuarine systems that can loose their connection to the sea (temporarily open-closed estuaries, Whitfield, 1992) and shallow lakes prone to evaporation and rainfall can strongly vary in their depth, particularly in climatic areas that experience distinct dry and wet seasons (tropics and subtropics) or dry and wet periods on longer time scales. Further, resuspension of sediment due to tidal activities or wind leads to variability in underwater light availability on time scales of hours (tides) and days (e. g. alternation of calm and windy days). In systems where both the water depth and turbidity vary in time or space primary production may be highly variable (e. g.

* Corresponding author.
E-mail addresses: katrintirok@gmail.com, tirok@ukzn.ac.za (K. Tirok).

http://dx.doi.org/10.1016/j.ecss.2014.05.011
0272-7714/

MacIntyre and Cullen, 1996) influencing food availability for higher trophic levels. Understanding what drives different patterns in primary production is important to understand the flow of energy through food webs and the dynamics of food webs (Miller et al., 1996; Jassby et al., 2002).

It is well known that primary production varies seasonally and spatially (e. g. Jassby et al., 2002; Perissinotto et al., 2010), however short term variability was identified to be important as well and there are still open questions in particular on the role of short-term variability on primary production at larger time scales, e. g. seasonal or annual production (Desmit et al., 2005; Canion et al., 2013). Long-term data sets often arise from monitoring schemes where samples are taken on bi-weekly to monthly or even less frequent time steps. While such data are invaluable for our understanding of primary production in aquatic systems, they do not allow for resolution of short-term variability. In addition to experiments at different time scales, mathematical models are useful tools for developing frame works and explore different scenarios. In this study we investigate the effect of the variability in both water depth and turbidity on primary production in a shallow coastal system with the aid of a dynamic simulation model, motivated by observations from an estuarine lake system, Lake St. Lucia (South Africa).

Lake St. Lucia, South Africa's first World Heritage Site, is a shallow and turbid estuarine lake system situated on the East Coast of South Africa (Cyrus, 1988) providing 80% of the estuarine area in KwaZulu-Natal and 50% of that in South Africa. Wet and dry periods occur on decadal time scales, therefore periods with low rainfall spanning several consecutive years are common for the St. Lucia catchment (Lawrie and Stretch, 2011). During the last decade, between 2002 and 2011, below average rainfalls led to drastically reduced water levels and desiccation of the lake of up to 90% was observed in some years (Whitfield and Taylor, 2009; Cyrus et al., 2010). The lack of freshwater entering the system was also intensified by the artificial separation of the Mfolozi river from the St. Lucia inlet which took place in the early 1950s to prevent increasing silt loads reaching the lake system (Day et al., 1952; Taylor, 1982). Lake St. Lucia is classified as highly turbid with turbidities >80 NTU (Cyrus, 1988). Wind is the driving force leading to resuspension of sediment and thus high turbidities in the large and shallow lake (Cyrus, 1988; Pringle, 2011). Turbidity is highly variable from day to day, and between seasons due to variable wind conditions (Cyrus, 1988). Perissinotto et al. (2010) suggest that primary production in Lake St. Lucia is mainly light limited given high turbidities, but high algae biomasses in certain areas might result from shallow water depths. It is unlikely that nutrient limitation inhibits algae growth since low nutrient levels were rarely observed (Perissinotto et al., 2010; Van der Molen and Perissinotto, 2011). Van der Molen and Perissinotto (2011) showed that microalgae production in Lake St. Lucia is mainly influenced by salinity, irradiance (as photosynthetic active radiation close to the bottom of the water column), and temperature. Their results indicate that light availability in the water column and thus turbidity plays an important role in influencing the dynamics of primary production in Lake St. Lucia which motivated our theoretical study on the effects of variable turbidities in connection with variable water depths on seasonal primary production of microalgae.

This theoretical study aimed to investigate the interrelated effects of water depth and turbidity on seasonal microalgae production in very shallow and turbid systems such as Lake St. Lucia. We emphasise the temporal variability of water depth and turbidity to provide a framework for present and future studies and inform management decisions. First, we investigated field data of turbidity and water depth from Lake St. Lucia from 2005 to 2011 to establish empirical ranges of these variables and their variability and calculated the relative light availability in the water column and at the bottom of the water column. Second, we used a mathematical model to simulate the dynamics of microalgae in relation to light availability (global irradiance, water depth, turbidity/light attenuation), nutrients, salinity, and temperature. We ran a set of simulations with different water depths and turbidity distributions, then compared the seasonal microalgae production of the different scenarios.

2. Methods

2.1. Study site and field data

The St. Lucia estuarine lake system is situated on the northern east coast of South Africa between 27° 52′–28° 24′ S and 32° 21′–32° 34′ E. The system consists of three shallow interconnected lake basins (South Lake, North Lake, False Bay) linked to the Indian Ocean via a 21 km long natural channel, the Narrows (Fig. 1). The system covers an estimated 300–350 km^2, depending on water levels (Cyrus, 1989; Taylor, 2006) and has an average depth of 1 m. Thus the lake is sensitive to direct rainfall inputs and evaporative losses. In times of very low rainfall, losses from the system exceed inputs.

Water depth and turbidity were measured quarterly as part of a basic monitoring program, at 5 different stations in the lake (Fig. 1) — the Estuary Mouth (MT), the Narrows (ES), Catalina Bay on the eastern shores (CB) and Charters Creek on the western shores of South Lake (CC), as well as Listers Point at False Bay (LP) from August 2005 until May 2011. Turbidity (NTU) was measured using either a YSI 556 or YSI 6920 Multiprobe system, in the top 20 cm of the water column and at the bottom of the water column at sites deeper than 50 cm. Depth averaged values were used for further calculations. Stratification was not observed due to vertical mixing driven by wind-wave generated turbulence. Depth was measured with a ruler when very shallow (<0.5 m), otherwise it was taken from YSI readings. Depth was measured approximately 50–100 m from the shore at CC, CB, and LP, and from the boat in the middle of the Narrows at ES. These depth measurements represent the water depth at each sampling site, but do not represent the mean water level of the subsystem. However, they represented changes in the water level at each site and served as a proxy for the entire lake area. Their representativeness was assumed due to the shallow depths throughout the lake basins (e. g. MacKay et al., 2010). There are no representative depth measurements for the Mouth because sampling was conducted from the shore, but total depth usually exceeds 2 m (e. g. MacKay et al., 2010). Photosynthetic active radiation (PAR, 400–700 nm) and turbidity were additionally measured at CC, LP, and MT biweekly from October 2010 until July 2011 to establish a relationship between turbidity and light attenuation in the lake system. Surface and bottom PAR were measured using an LI-COR light meter, fitted with an LI-193SA spherical quantum sensor. These measurements were used to calculate the diffusive light attenuation coefficient (κ, Kirk, 1994), using the following equation: $\kappa = -ln(I_{z2}/I_{z1})/(z2-z1)$, where I_{z2} is radiation (μmol photons m^{-2} s^{-1}) at depth $z2$ (m) and I_{z1} is radiation at depth $z1$. A linear regression model between log transformed turbidities and log transformed light attenuation coefficients resulted in: $log(\kappa) = 0.78 \cdot log(turb) - 0.72$, $r^2 = 0.82$, $p < 0.01$ (Fig. 2 D). This model was used to estimate κ from measured or simulated turbidities, which was subsequently used in the calculations of light availability and primary production.

2.2. Relative light availability

To obtain information on potential light limitation or photoinhibition of microalgae production in Lake St. Lucia, the relative

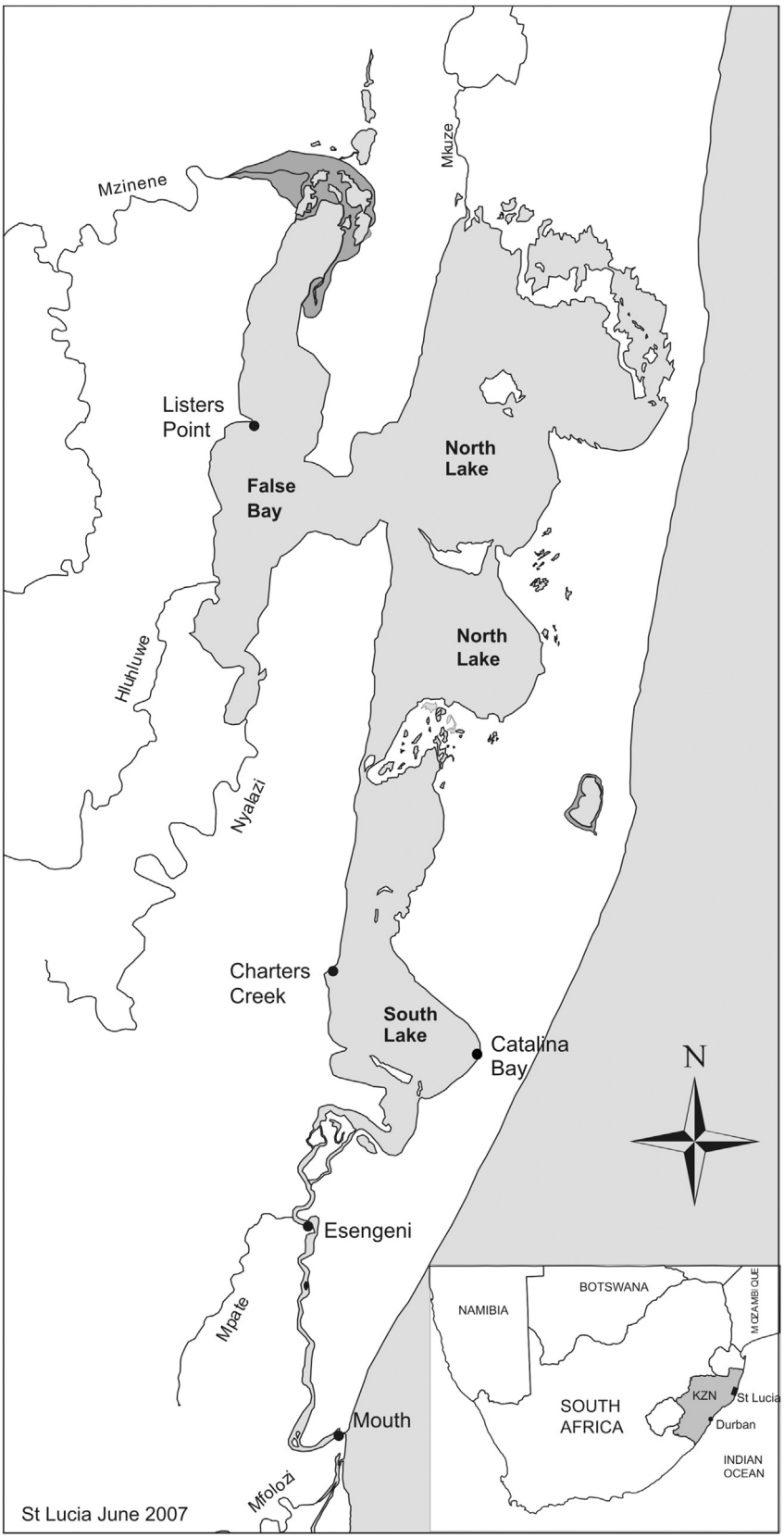

Fig. 1. Map of Lake St. Lucia with the sampling sites indicated by black circles. Provided by Sarah Bownes, created from data captured by the U.S. Geological Survey, Centre for Earth Resources Observation and Science (EROS) (http://edcsns17.cr.usgs.gov/NewEarthExplorer).

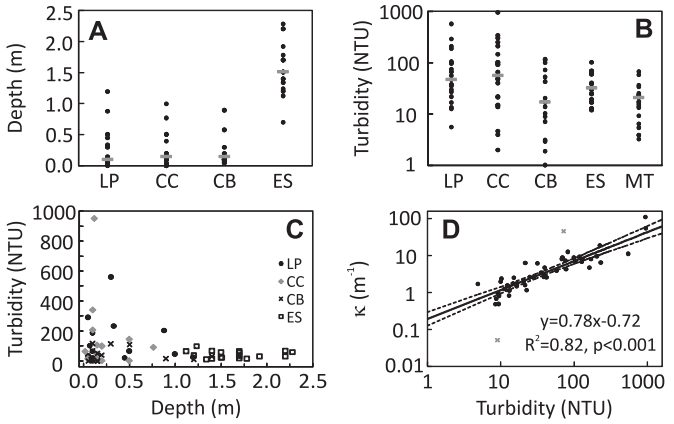

Fig. 2. Observed water depths (**A**) and turbidities (**B**) at different sampling sites in Lake St. Lucia between August 2005 and May 2011 (quarterly data), showing a high variability during the recent drought. For the Mouth representative depth measurements were not available. Each black dot represents one data point, grey bars represent the medians. (**C**) Relationship between water depth and turbidity. The highest values of turbidity were observed at the lowest water depths. (**D**) Relationship between light attenuation coefficient (κ) and turbidity with linear model and 95% CI (biweekly data from October 2010–July 2011 from LP, CC, and MT). Grey crosses mark outliers not included in the model (z-score of residuals $>|2.5|$, $n = 50$).

light availability in the water column (rI_m, Eq. (1)) and at the bottom of the water column (rI_d, Eq. (2)) was calculated as a fraction of surface radiation (I_0) from observed combinations of light attenuation (estimated from turbidity using the linear regression model, cf. Fig. 2) and water depth for the sites ES, CB, CC, and LP from 2004 to 2011.

Relative light availability averaged over the water column:

$$rI_m = \frac{I_m}{I_0} = \frac{\left(1 - e^{(-\kappa \cdot d)}\right)}{\kappa \cdot d} \quad (1)$$

Relative light availability at the bottom of the water column:

$$rI_d = \frac{I_d}{I_0} = e^{-\kappa \cdot d} \quad (2)$$

with d = total depth (m) and κ = light attenuation coefficient (m^{-1}) estimated from turbidity measurements (Fig. 2). A value of $rI_d = 0.01$ means that the total depth corresponds to the euphotic depth, therefore values greater than 0.01 indicate that the entire water column was euphotic.

2.3. Mathematical model

We developed a mathematical model to simulate the effect of different water levels as well as different levels and variabilities of turbidity on seasonal primary production of pelagic and benthic microalgae.

2.3.1. Model description

The model describes the temporal dynamics of pelagic and benthic microalgae and their nutrient cell quota (cf. "Droop model", Droop, 1983), as well as of nutrients in the water column and in the pore water. The changes in biomass, nutrients, and cell quota over time are calculated by solving a set of coupled differential equations. Biomass of microalgae (B, mg C m^{-2}) increases due to production and decreases due to respiration, mortality, and grazing and can be written as: dB/dt = +production − (respiration + mortality + grazing) (cf. Eq. (A.1) in Appendix A). The cell quota (Q, -) changes due to uptake of nutrients and consumption by production: dQ/dt = +uptake − production (cf. Eq. (A.2)). Dynamics of nutrients (N, mg m^{-2}) depend on nutrient uptake and nutrient remineralisation: dN/dt =+ remineralisation−uptake (cf. Eqs. (A.3), (A.4)). All detailed equations are given in the Appendix A. A description and the values of parameters are given in Table 1. Equations for the individual processes are mainly based on previously used formulations and known relationships (see reference to equations in main text and Appendix A). Thereafter, the differential equations incorporating the various processes were developed.

We did not distinguish between different taxonomic groups, but between two fractions, a pelagic and a benthic one. We did not account for sedimentation of pelagic microalgae or resuspension of benthic microalgae. We rather assumed that algae in the pelagic fraction contain algae that are regularly deposited and resuspended, whereas algae in the benthic fraction are such species avoiding to be resuspended. In shallow waters algae in the water column often contain species classified as benthic (Nche-Fambo, 2014), further some benthic species are able to vertically migrate within the sediment and may avoid resuspension (Mitbavkar and Anil, 2004). In our model, the equations for the pelagic and the benthic fraction differ only in the assumption that the benthic fraction can utilize both water column and pore water nutrients (Eq. (A.11)), whereas the pelagic fraction rely solely on water column nutrients (Eq. (A.10)).

Primary production, nutrient uptake, respiration, mortality and grazing depend on light, nutrients, temperature and salinity (for details see Appendix A, Eqs. (A.5)-(A.11), (A.17-A.21), (A.26), (A.29)). Light-dependent production is calculated per hour and summed over the day. Therefore, shorter days have a reduced light dependent production rate. The production of pelagic algae per hour is averaged over the water column (Eq. (A.23)), while the production of benthic microalgae per hour is calculated at the bottom of the water column (Eq. (A.29)). It was assumed that benthic primary production is saturated at a lower light intensity than pelagic production (Eqs. (A.27), (A.30), Table 1).

Nutrient dependent production and nutrient uptake is modelled using the Droop model (Droop, 1983), i. e. nutrient uptake and production are decoupled and both are linked to the internal cell quota (Eqs. (A.5), (A.10), (A.11), (A.17)). The total amount of nutrients (N_{tot}, mg N m^{-2}) remains constant throughout the simulations. The volumetric nutrient concentration in the water column is calculated based on the water depth for each simulation step, i. e. a lower water depth can lead to a higher nutrient concentration if the amount of nutrients bound in algae and in the sediment is constant. Similarly, Johnson (1977) reported that nutrient poor freshwater inflows (direct rainfall or river inflow) lead to higher water levels which result in low nutrient concentrations in the water column in parts of Lake St. Lucia due to dilution. N_{tot} consists of dissolved nutrients in the water column, dissolved nutrients in the pore water, nutrients bound in pelagic and benthic microalgae, and other particulate nutrients (e. g. detrital nutrients). The latter corresponds to the difference between N_{tot} and the dissolved nutrients, and nutrients bound in algae. The nutrient dynamics are highly simplified in the model and do not include sediment specific nutrient processes, but resolve pore water nutrients as an additional nutrient source for benthic algae.

Grazing by zooplankton and macro-zoobenthos is represented implicitly by a dynamic grazing rate for microalgae (Eq. (A.9)). The dynamic grazing rate depends on the previous algal concentration including a time delay, which represents the lag in development of grazers when compared to algae (Tirok and Gaedke, 2007). Therefore, predator dynamics and thus their grazing pressure follow their prey with a time lag of 14 days in our model. This

Table 1
Full list of model parameters. PA: pelagic algae, BA: benthic algae, wc: water column, pw: pore water.

Parameter	Symbol	Value	Unit	Reference
Potential growth rate of pelagic algae	r^0_{PA}	0.17	h^{-1}	Adjusted, Reynolds (2006)
Potential growth rate of benthic algae	r^0_{BA}	0.05	h^{-1}	Adjusted
Potential activity dependent respiration rate	a^0	0.2	d^{-1}	Geider (1992)
Potential basal respiration rate	b^0	0.05	d^{-1}	Baretta et al. (1995)
Potential mortality rate for pelagic algae	m^0_{PA}	0.02	d^{-1}	Estimated
Potential mortality rate for benthic algae	m^0_{BA}	0.02	d^{-1}	Estimated
Density dependent mortality parameter for pelagic algae	g^0_{PA}	0.05	$(mg\ C\ m^3)^{-\alpha}\ d^{-1}$	Estimated
Density dependent mortality parameter for benthic algae	g^0_{BA}	0.01	$(mg\ C\ m^3)^{-\alpha}\ d^{-1}$	Estimated
Exponent for density dependent mortality	α	0.5	–	Estimated
Time delay in density dependent mortality	τ	14	d	Estimated
Maximum nutrient uptake rate of pelagic algae	v^0_{PA}	1	$mg\ N\ (mg\ C)^{-1}\ d^{-1}$	Adjusted, Reynolds (2006)
Maximum nutrient uptake rate of benthic algae	v^0_{BA}	1	$mg\ N\ (mg\ C)^{-1}\ d^{-1}$	Adjusted
Half-saturation constant for nutrient uptake of pelagic algae	k_{PA}	25	$mg\ N\ m^{-3}$	Adjusted, Reynolds (2006)
Half-saturation constant for nutrient uptake of benthic algae	k_{BA}	50	$mg\ N\ m^{-3}$	Adjusted
Minimum nutrient cell quota	q_{min}	0.04	mg N : mg C	Sommer (1991)
Maximum nutrient cell quota	q_{max}	0.4	mg N : mg C	Sommer (1991)
Proportion of photosynthetic active radiation (PAR) of global irradiance	q_{PAR}	0.45	–	Kirk (e. g. 1994)
Minimal light intensity of saturated photosynthesis for pelagic algae	$I^{min}_{opt\_PA}$	150	µmol photons $m^{-2}\ s^{-1}$	Lampert and Sommer (1997), Reynolds (2006)
Minimal PAR of saturated photosynthesis for benthic algae	$I^{min}_{opt\_BA}$	50	µmol photons $m^{-2}\ s^{-1}$	Lampert and Sommer (1997), Reynolds (2006)
Maximal PAR of saturated photosynthesis for pelagic algae	$I^{max}_{opt\_PA}$	600	µmol photons $m^{-2}\ s^{-1}$	Lampert and Sommer (1997), Reynolds (2006)
Self shading coefficient	κ_P	0.0005	$m^{-2}\ (mg\ C\ m^{-3})^{-1}$	Krause-Jensen and Sand-Jensen (1998)
Optimum temperature for primary production and grazing	T_{opt}	26	°C	Estimated
Strength of temperature effect for primary production	h_{ta}	0.004	$(°C)^{-2}$	Arhonditsis and Brett (2005)
Strength of temperature effect for grazing	h_{tg}	0.01	$(°C)^{-2}$	Estimated
Q_{10} Value for heterotrophic processes	Q_{10}	2.0	–	General textbook
Reference temperature	T_{ref}	20	°C	
Minimum salinity for optimal growth	S_{min}	5	–	Johnson (1977)
Maximum salinity for optimal growth	S_{max}	50	–	Johnson (1977)
Exponent for salinity optimum curve	β	2	–	Griffin et al. (2001)
Total nutrient concentration	N_{tot}	1000	$mg\ N\ m^{-2}$	Estimated from Perissinotto et al. (2010)
Remineralisation rate of particular nutrients	z	0.35	d^{-1}	Adjusted, Huber et al. (2008)
Diffusion rate of pore water nutrients into water column	δ	0.002	d^{-1}	Estimated

grazing rate predominantly represents grazing by crustaceans (copepods, mysids, Carrasco and Perissinotto, 2010; Jerling et al., 2010) as well as benthic invertebrates (Pillay and Perissinotto, 2008, 2009; MacKay et al., 2010) which both feed on pelagic and benthic microalgae (Carrasco and Perissinotto, 2010; MacKay et al., 2010). Benthic and epiphytic microalgae also provide a food source for some fish species (e. g. mugilids, *Oreochromis mossambicus*) in Lake St. Lucia (Whitfield et al., 2006). We assumed that pelagic algae experience a higher grazing pressure than benthic algae because algae in the water column are more strongly affected by efficient filter feeders. One of the most important filter feeders in Lake St. Lucia during 2005–2011 was *Solen cylindraceus* (Pillay and Perissinotto, 2008; MacKay et al., 2010; Nel, 2011).

The simulation model is driven by time-series of water depth, turbidity, global irradiance, salinity, and water temperature. Turbidity values were converted to a light attenuation coefficient K_{sed} using the linear model given in Section 2.1 Study site and field data which represents light attenuation due to suspended material except algal biomass in our model. The overall light attenuation coefficient (κ) is the sum of K_{sed} and light attenuation due to pelagic algae biomass, $\kappa_P \cdot B_{PA\_vol}$, (Eq. (A.16)). Daily Global Irradiance of the years 2000–2010 was obtained from SASRI weather web (http://portal.sasa.org.za/weatherweb, station "Hluhluwe–Glenpark"). We randomly chose one year from the years 2000–2010 in each model run (cf. 2.3.2 Simulation runs) to account for the variability in irradiance between years. From these daily irradiances hourly values were calculated for each day of the year depending on the photoperiod of that day according to the geographical latitude of Lake St. Lucia (28° S, cf. Section A.5 Calculation of irradiance per hour in Appendix A). Salinity was assumed to change with water depth. The total amount of salt was set to 10 kg m^{-2} which corresponds to salinity of 10 for a water depth of 1 m, and 50 for a water depth of 0.2 m. These values represent the observed range of salinities in Lake St. Lucia, but exclude extreme values of up to 250 which occurred occasionally (MacKay et al., 2010; Perissinotto et al., 2010). Daily water temperature was simulated using a sine type function (cf. Eq. (A.37)), with a minimum and maximum value of 15 °C in winter and 30 °C in summer, respectively. Minimum and maximum temperatures correspond to observed values in the system in the different seasons (e. g. MacKay et al., 2010). In this simple approach we did not include the influence of water depth on temperature.

2.3.2. Simulation runs

Three different water depth scenarios were simulated, (i) constant water depth throughout a year, (ii) "normal" seasonal trend with decreasing water depth in winter and increasing depth in summer as observed in Lake St. Lucia in response to rainfall patterns, and (iii) "reversed" seasonal trend with increasing depth in winter and decreasing depth in summer (Fig. 3). For these three scenarios different water depths were used, 0.2–1.2 m in steps of 0.2 for (i), and average water depths of 0.4, 0.6, and 0.8 m with a range of 0.4 m for (ii) and (iii) (Fig. 3). Daily values of turbidity were obtained as random numbers from different log-normal distributions. Different mean values (log_{10} of 5, 10, 20, 40, 60, 80, 120, and 200 NTU, in the following referred to as μ_{turb}) as well as different standard deviations (0.15, 0.3, 0.6, and 1.2, referred to as σ_{turb}) for each μ_{turb} were tested (Fig. 4). These values cover the range of

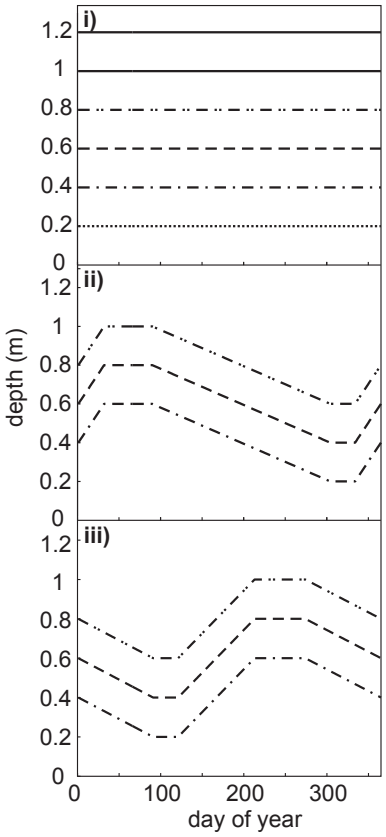

Fig. 3. Different depth scenarios used in the model simulations. **(i)** constant depths, **(ii)** seasonally varying depths with "normal" seasonal trend, and **(iii)** seasonally varying depths with "reversed" seasonal trend.

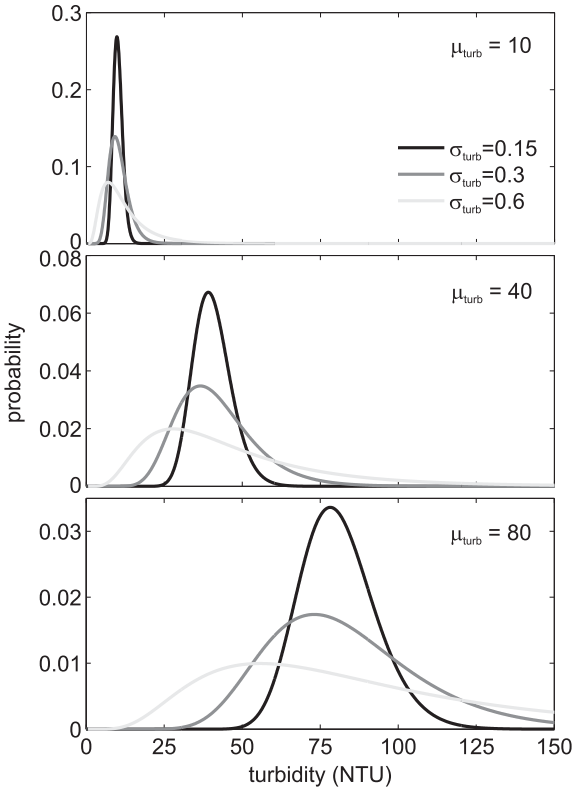

Fig. 4. Examples of log-normal probability distributions of turbidity used in the model simulations, μ_{turb} —mean value, σ_{turb} —standard deviation, see 2.3.2 Simulation runs in Methods for details.

observed distributions in Lake St. Lucia (μ_{turb}=17–51 NTU, σ_{turb}=0.27–0.68, Table 2 in the Results) and also take lower and higher turbidities into account. For each combination of water depth, mean turbidity, and standard deviation of turbidity, 50 runs were simulated for a duration of one year each. For every run the net production of pelagic and benthic algae was calculated and summed for summer (October–March) and winter (April–September) and then averaged over the 50 runs. Furthermore, we calculated the average biomass of pelagic and benthic algae and the balance between pelagic and benthic production and biomass over summer and winter, and over the 50 runs. The balance of pelagic versus benthic production and biomass was calculated as percentage of total gross production and percentage of total biomass, respectively.

To investigate the influence of varying water depth on seasonal production, we calculated the percentage change and its error (Eqs. (3) and (4)) from model scenarios with constant depths of 0.4, 0.6, and 0.8 m (depth scenario (i), x_1 in Eq. (3)) to scenarios with varying water depth with the mean values of 0.4, 0.6, and 0.8 m (depth scenario (ii), (iii), x_2 in Eq. (3)).

$$\Delta x = 100 \cdot \frac{(x_2 - x_1)}{x_1} \tag{3}$$

$$s_{\Delta x} = 100 \cdot \frac{x_2}{x_1} \cdot \sqrt{\left(\frac{s_{x2}}{x_2}\right)^2 + \left(\frac{s_{x1}}{x_1}\right)^2} \tag{4}$$

x_1–result from reference simulation, x_2–result from alternative simulation, s–standard error

All simulations, calculations and plotting were done in MATLAB 7.x R2009b (The MathWorks). Our overall aim was a general theoretical study on the interrelated effects of variable water depth and turbidity for seasonal microalgae production which was inspired by conditions in Lake St. Lucia. Thus, we did not explore a parametrisation and validation with specific data from Lake St. Lucia, but compared the simulated annual production to observations from Lake St. Lucia and other systems. Further, we looked at the effect of photoinhibition in our model in more detail and we conducted a sensitivity analysis to determine to what extent the model is influenced by the parameters defining light adaptation compared to growth/grazing parameters (see Appendix B for details).

3. Results

3.1. Field data of water depths and turbidities

Measured water depths at different sampling sites indicate a high variability of both the mean lake water level during

Table 2
Parameters of log-normal distributions (log-mean = mean of $\log_{10}(turb)$, log-std = standard deviation of $\log_{10}(turb)$), median, and arithmetic mean (mean) of turbidities (NTU) in Lake St. Lucia during 2005–2011.

Site	log-mean	log-std	$10^{log-mean}$	Median	Mean	*n*
LP	1.71	0.50	51	47	97	20
CC	1.64	0.68	43	56	135	22
CB	1.26	0.64	18	17	42	19
ES	1.56	0.27	36	32	42	21
MT	1.23	0.36	17	21	22	22
All	1.48	0.55	31	31	67	104

2005–2011 and the daily water level at the sampling site due to wind driven water movements (Fig. 2). The depth varied between 0 and 1.2 m in the lake basins (LP, CC, CB) and between 0.7 and 2.3 m in the Narrows (ES). In some seasons, parts of the lake were desiccated, whereas during the period with the mouth open in 2007 the water depths were highest, with about 1 m in the lake basins, and more than 2 m in the Narrows. Turbidities were generally high, with medians between 17 (CB) and 56 NTU (CC). Values above 100 NTU were frequently observed in the lake basins (CC, LP, and CB), whereas turbidities remained below 100 NTU at ES and MT. The highest turbidities, with values up to 950 NTU, occurred at the lowest water depths at CC and LP (Fig. 2 C). The turbidity values followed a log-normal distribution with high variabilities (Table 2). Turbidity was strongly correlated with the light attenuation coefficient (κ, Fig. 2 D). High turbidities of >150 NTU corresponded to light attenuation coefficients of $\geq$10 m^{-1}, i. e. a strong reduction of light availability in the water column. The main source of high turbidity was suspended silt from largely fine sand and muddy sediment in Lake St. Lucia, whereas water column chl *a* (microalgae) was of minor importance. Chl *a* in the water column contributed less than 10% to the total light attenuation coefficient in the lake basins on most of the sample days, whereas in the St. Lucia Mouth, chl *a* contributed between 10 and 36%. These calculations were based on chl *a* measurements in Lake St. Lucia (data from Perissinotto et al., 2010) and a chl *a* specific attenuation coefficient of 0.015 m^2 (mg chl *a*)$^{-1}$ (Krause-Jensen and Sand-Jensen, 1998).

Overall, light availability in the lake basins (LP, CC, CB) was high due to low water depth despite high turbidities. On average 65–95% of surface radiation was available in the water column and 40–90% was available at the bottom of the water column. In the deeper Narrows, light availability was lower than in the lake basins with less than 20% of surface radiation available in the water column and less than 1% available at the bottom of the water column. Given these field observations, light limitation probably played a minor role in the lake basins during the years 2005–2011 when water levels were very low. However, in the deeper Narrows and during periods with higher water levels in the lake basins, light limitation likely reduced primary production.

3.2. Model simulations

Simulations with the mathematical model were run for one year and repeated 50 times. In the simulations the water depth was either constant or varied with seasons (cf. Fig. 3). The average daily turbidity was chosen randomly from log-normal distributions differing in their mean values (μ_{turb}) and standard deviations (σ_{turb}, cf. Fig. 4). This allowed us to test the effect of different absolute levels of turbidity on primary production combined with the effect of different day-to-day variability of turbidity within one year.

When the water depth is constant throughout the year, patterns of primary production for different depths and turbidities indicate that light was the main factor determining microalgae dynamics in the model. Total net production was higher in summer than in winter, and it decreased with increasing depth and with increasing mean turbidity (Fig. 5). The same holds for the seasonal average standing stock. At very low water depths, the seasonal production

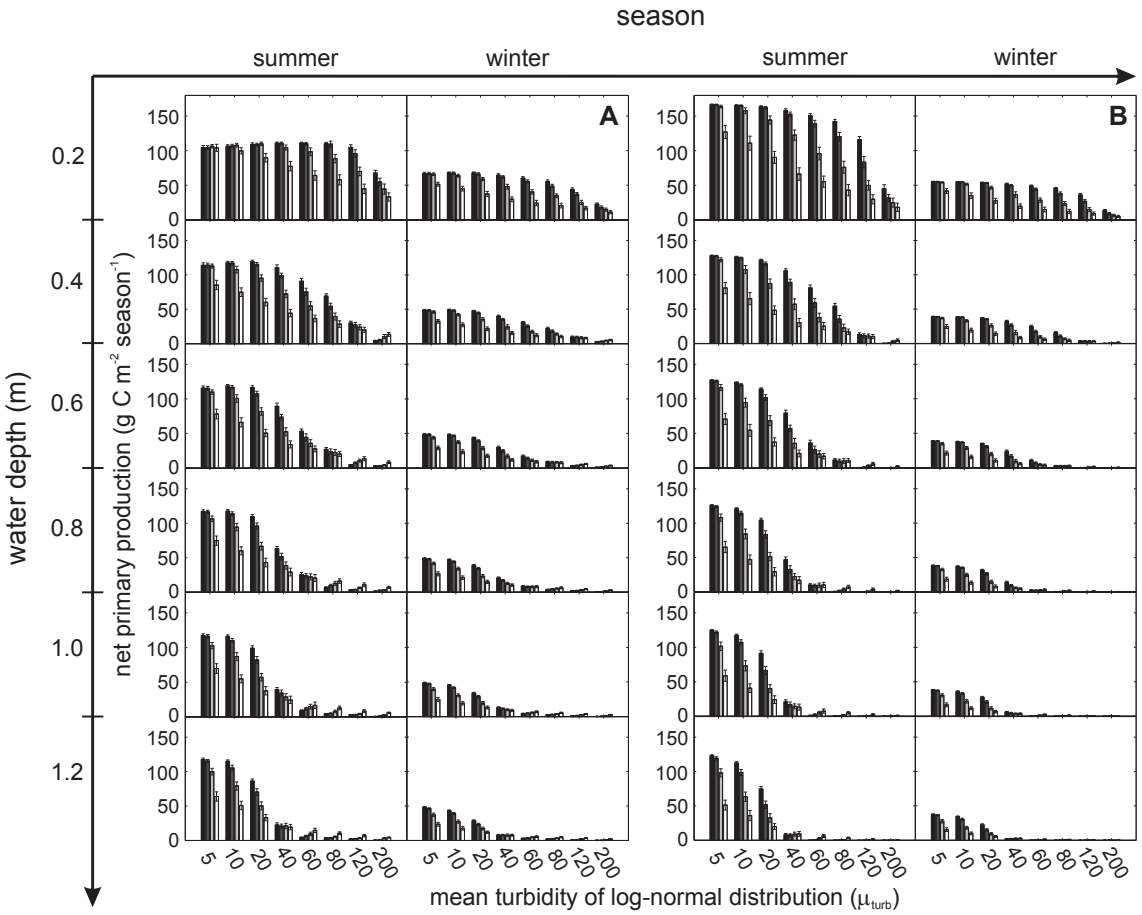

Fig. 5. Summed net primary production of pelagic (**A**) and benthic microalgae (**B**) in summer and winter for different mean turbidities (x-axis) and different water depth (outer y-axis, panels from top to bottom). Bars with error bars show mean values of 50 model runs with standard deviations. Shading of the bars corresponds to the different probability distributions of turbidity, black: σ_{turb} = 0.15, dark grey: σ_{turb} = 0.3, light grey: σ_{turb} = 0.6, white: σ_{turb} = 1.2. For details see methods and Fig. 4.

of microalgae was only lowered when mean turbidities were high (≥80 NTU). At higher depths seasonal production was considerably lowered at mean turbidities of ≥40 NTU. This pattern was the same in summer and winter and for both the pelagic and benthic fraction.

Different day-to-day variabilities of turbidity values within a year led to strongly different seasonal production in some cases. The extent and direction of the effect of variability of turbidity depended on the water depth and the mean turbidity (μ_{turb}). In shallow water as well as at low mean turbidities, seasonal production decreased with increasing variability of turbidity, i.e with an increasing range of turbidity values within a year (Fig. 5). This effect was due to the high number of very turbid days in a wide distribution compared to a narrow one. For example, at $\mu_{turb} = 60 - 120$, the turbidity exceeded 500 NTU at 23 – 55 days per year when $\sigma_{turb} = 0.6$, compared to 1 – 7 days per year when $\sigma_{turb} = 0.3$. On the contrary, in deeper water, when the mean value of turbidity was already high (≥60 NTU), the higher number of less turbid days in a wide compared to a narrow distribution enhanced the seasonal production (Fig. 5). At $\mu_{turb} = 60 - 120$, turbidity was less than 20 NTU at 35 – 78 days per year when $\sigma_{turb} = 0.6$, compared to 2 – 20 days when $\sigma_{turb} = 0.3$. This means that days with high and low turbidity did not simply counteract each other in their effect on seasonal production.

The balance between pelagic and benthic gross production and biomass showed differences at different water depths and mean turbidities. The benthic fraction contributed slightly more than 50% to the total microalgae gross production, and more than 75% to total microalgae biomass in shallow water and at low turbidities (Fig. 6). This balance was also influenced by the variability of turbidity. The pelagic algae fraction dominated production at high water depth and at high turbidities with little variability whereas both fractions reached an equal share in gross production at high turbidities with high variability (Fig. 6). Since light was the main factor determining primary production in the model the balance between the pelagic and benthic algae fraction also depends on the formulation and parameters chosen for the P–I curve. For results with changed parameters of the P–I curves see Appendix B.

Water depth in Lake St. Lucia varied strongly within a given year during the period 2005–2011 depending on rainfall and evaporation. We compared the seasonal net production of simulated years with constant water depth (scenario (i)) with that of simulated years with varying water depth (scenario (ii), (iii), cf. Fig. 3). Potential changes in production due to varying water depth within a year compared to constant water depth depended strongly on the combination of depth, mean turbidity as well as variability of turbidity. For mean turbidities up to 60 NTU, no or little differences in production were predicted between runs with constant and varying water depth (Fig. 7). For higher turbidities, high differences in production occurred, with the highest differences observed in benthic production. At high turbidities small changes in water depth resulted in the

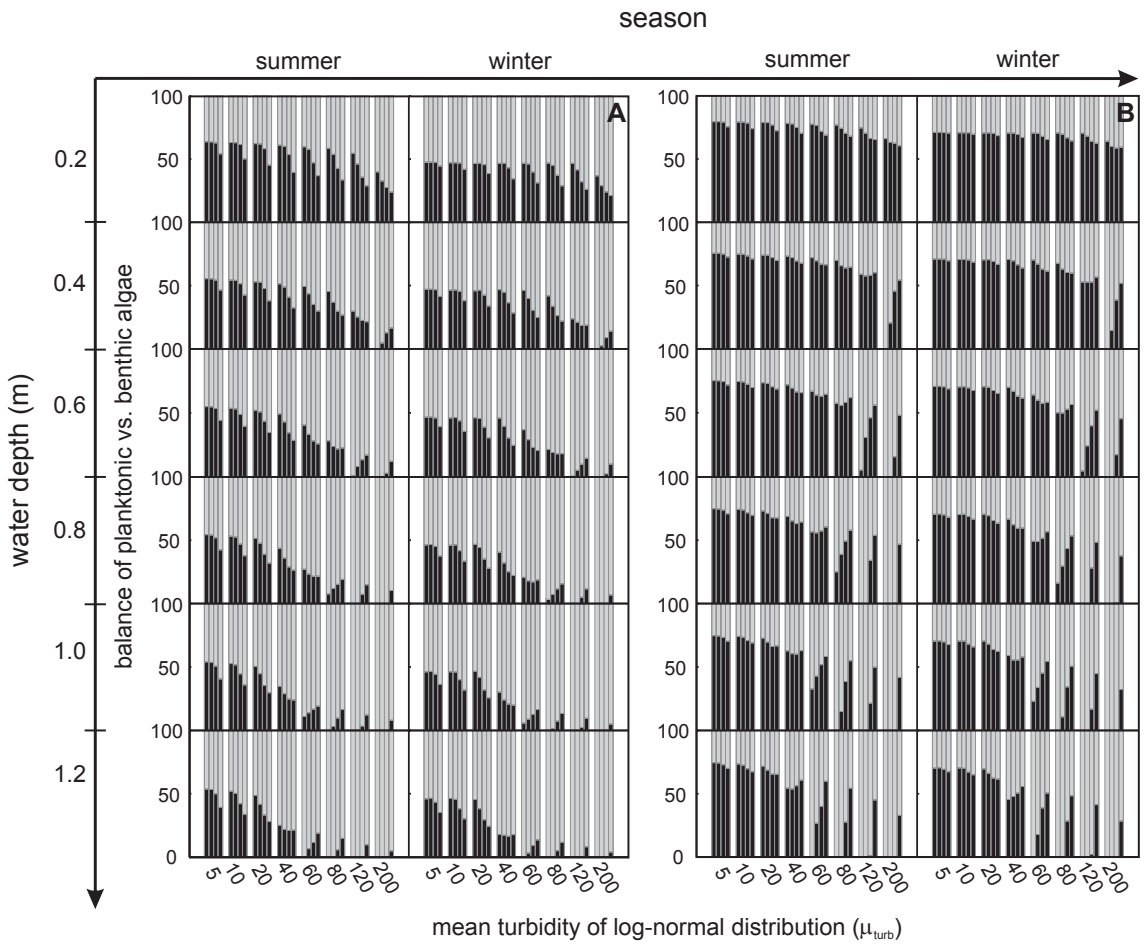

Fig. 6. Balance between pelagic (grey) and benthic algae (black) as percentage of total algal gross-production (**A**) and biomass (**B**) in summer and winter for different mean turbidities (x-axis) and different water depth (panels from top to bottom). Different variability in turbidity indicated by same position of bars as in Fig. 5.

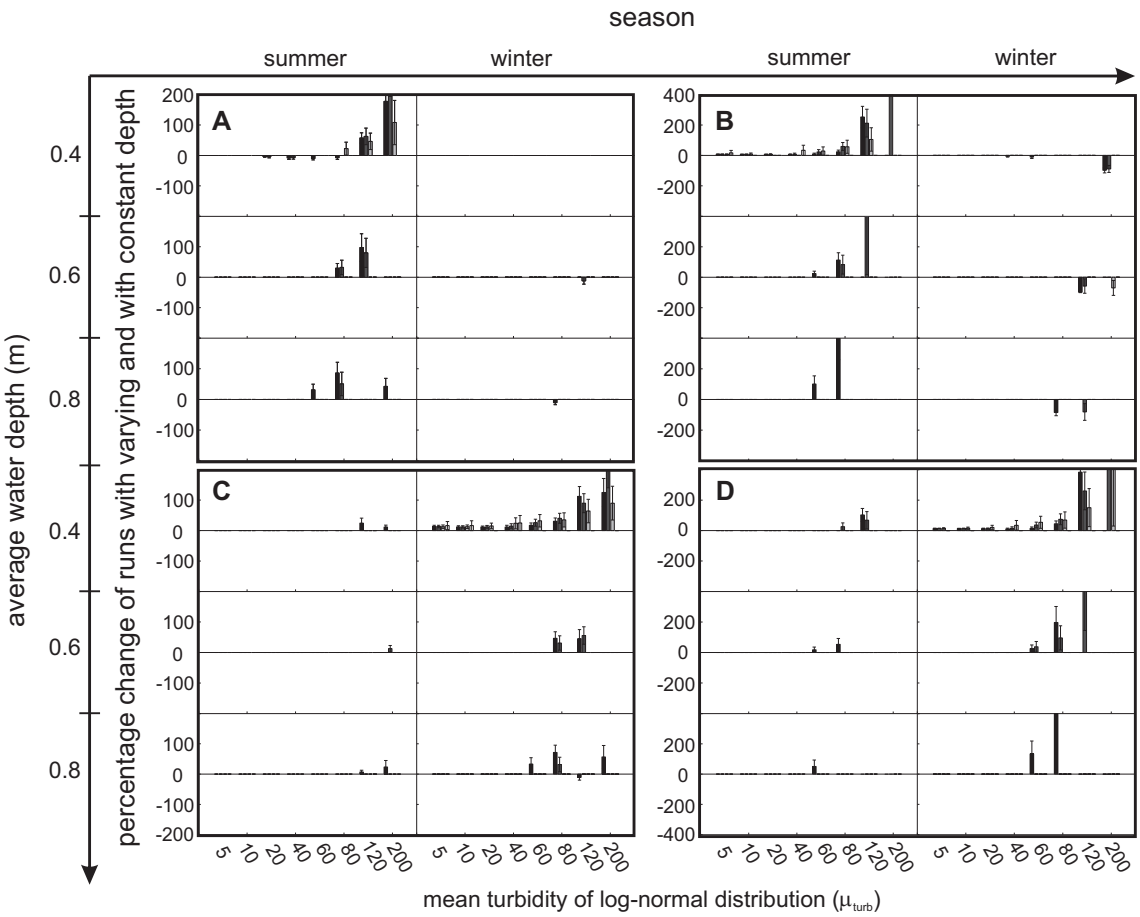

Fig. 7. Percentage change between net primary production of depth scenario (i) and (ii) (**A, B**) and depth scenario (i) and (iii) (**C, D**) of pelagic (**A, C**) and benthic microalgae (**B, D**) in summer and winter (cf. Fig. 3 for depth scenarios). Shading of bars as in Fig. 5. Note the different y-scales of differences in pelagic and benthic production. When the error of the difference was larger than the absolute value of the difference, differences were not plotted. Differences $>|200|$% for pelagic algae and $>|400|$% for benthic algae were cut off.

underwater light availability changing between limiting and saturating conditions. For highly variable turbidities ($\sigma_{turb} = 1.2$), seasonal production did not differ between the different depth scenarios.

In simulated years when the water depth followed the "normal" seasonal trend, i. e. decreasing in winter and increasing in summer (depth scenario (ii), cf. Fig. 3), the model predicted an enhanced production at high turbidities (≥80 NTU) in summer (Oct–Mar), but not in winter (Apr–Sep) compared to years with constant depth (scenario (i)) (Fig. 7 A, B). When the water depth followed the "reversed" seasonal trend, i. e. increasing in winter and decreasing in summer (depth scenario (iii), cf. Fig. 3), the pattern was more or less reversed. Production was enhanced at high turbidities in winter, but not in summer (Fig. 7 C, D).

Mean turbidities observed in Lake St. Lucia in 2005–2011 were 20–60 NTU (cf. Table 2). They correspond to the medium range of the mean turbidities tested in our model. For these values a varying water depth within a year barely resulted in a different production compared to a constant depth within a year. Thus, this study indicates that changes in the water depth within a year were unlikely to play a role for the annual production in Lake St. Lucia. However, large differences in the average water depth between individual years or during different (dry/wet) periods spanning several years are likely to lead to considerably higher or lower seasonal microalgae production as suggested by the simulations with different constant water depths.

3.3. Model validity

Simulated annual net production ranged between 0.3 and 177 g C m^{-2} $year^{-1}$ in the pelagic and between 0 and 222 g C m^{-2} $year^{-1}$ in the benthic subsystem over the entire range of the depth–turbidity combinations. Simulated average standing stocks ranged between 6 and 495 mg C m^{-2} in the pelagic and between 0 and 1606 mg C m^{-2} in the benthic subsystem. These values lie within the range of reported values of microalgae production and biomass in Lake St. Lucia as well as in other estuarine systems worldwide (Table 3). The highest values of production and biomass occurred at low turbidity and low depth and vice versa. This pattern corresponds with findings from Perissinotto et al. (2010, 2013).

P:B ratios calculated from the measurements in Van der Molen and Perissinotto (2011) using a chl *a*:C ratio of 0.02 reached ~1 d^{-1} for pelagic algae and less than 0.1 d^{-1} for benthic algae. The production rate of the pelagic fraction in our model was similar (~1 d^{-1}) to the one measured, but that of the benthic fraction was higher than the one measured with values mainly >0.1 and up to 0.4 d^{-1}. In our model, the higher production rate for the benthic fraction ensured their high production and biomass at low depth or turbidity (cf. B.2 Sensitivity analysis in Appendix B). Neither our model nor the production measurements by Van der Molen and Perissinotto (2011) accounted for resuspension of benthic microalgae, which could result in higher production of benthic algae

Table 3
Primary production and biomass in our model and in different estuarine systems.

Depth (m)	Turbidity (NTU)	Production	Biomass	Reference
Data from this study				
Pelagic algae				
0.2–1.2	5–200	0.34–177 g C m^{-2} $year^{-1}$ up to 94 mg C m^{-2} h^{-1} or 470 mg C $m^{-3}h^{-1}$	6-495 mg C m^{-2} 0.12–10 mg chl *a* m^{-2} or 0.1–50 μg chl *a* l^{-1}	this study, model simulations
Benthic algae				
0.2–1.2	0–211	0-222 g C m^{-2} $year^{-1}$ up to 323 mg C m^{-2} h^{-1}	0-1606 mg C m^{-2} 0–32 mg chl *a* m^{-2}	this study, model simulations
Field data from Lake St. Lucia				
Pelagic algae				
<0.2, average, inlet closed	3–75, range	0-180 mg C $m^{-3}h^{-1}$	2.4–84 mg chl *a* m^{-3} 23.3±39.1 mg chl *a* m^{-3}	Van der Molen and Perissinotto (2011), Perissinotto et al. (2010)
1, average, inlet open	up to 250	218–252 mg C $m^{-2}d^{-1}$	2.1–16 mg chl *a* m^{-3}	Fielding et al. (1991)
Benthic algae				
<0.2, average, inlet closed	3–75, range	0–34 mg C $m^{-2}h^{-1}$	3–>300 mg chl *a* m^{-2} 147 ± 332 mg chl *a* m^{-2} (range: 0-–>500)	Van der Molen and Perissinotto (2011) Perissinotto et al. (2010)
Data from systems worldwide				
Pelagic algae				
Biomass	1.1–22 mg chl *a* m^{-3}		McLusky and Elliott (2004), global	
Production	50–500 g C m^{-2} $year^{-1}$ to 105–1890 g C m^{-2} $year^{-1}$ (net production), median 185 g C m^{-2} $year^{-1}$		Montes-Hugo et al. (2004), estuaries Cloern et al. (2013), estuarine-coastal ecosystems worldwide	
Benthic algae				
Biomass	0.5–500 mg C m^{-2} 100 mg chl *a* m^{-2}		Anandraj et al. (2008), estuaries South Africa Narragansett Bay (USA), Lake and Brush (2011)	
Production	29–314 g C m^{-2} $year^{-1}$ 1–9 mg C $m^{-2}h^{-1}$ up to 450 mg C m^{-2} d^{-1}		Underwood and Kromkamp (1999), estuaries worldwide Blasutto et al. (2005), coastal Mediterranean lagoons Lake and Brush (2011), Narragansett Bay (USA)	

when suspended in the water column contributing to high benthic biomass in the field (MacIntyre and Cullen, 1996). From regular surveys on a biweekly to quarterly basis the quantitative effect of resuspension is difficult to estimate and measurements regarding resuspension of microalgae and of nutrients are necessary.

Our model did not show an increasing integrated water column production with increasing depth which stands in contrast to observations from other systems (e. g. Montes-Hugo et al., 2004). Reasons for this discrepancy lie in the total nutrient concentration, which was kept at the same value of 1000 mg N m^{-2} for all simulations and thus the volumetric nutrient concentration (mg N m^{-3}) was higher at low depth compared to high water depth (as observed by Johnson, 1977). Running the simulations with the same volumetric nutrient concentration of 1000 mg N m^{-3} for the different depths, resulted in increasing integrated pelagic production and biomass with increasing depth.

Overall, annual pelagic and benthic production simulated by our model resembled that of a number of different shallow systems worldwide (cf. Table 3). Thus, our model presents a useful tool for analysis of interrelated effects of turbidity and water depth on seasonal primary production. We further conducted a sensitivity analysis which showed that the model is much more sensitive to uncertainties in the growth and grazing parameters than to uncertainties in the P–I curves, which means that the questions tested with our model would be affected only to a comparatively small extent by more specific P–I curves (see Appendix B for details).

4. Discussion

Since microalgae productivity and biomass are dependent on adequate amounts of light, levels of turbidity are of utmost importance especially in shallow lakes and estuarine systems where resuspension of sediments and detritus quickly increase turbidity in the shallow water column. However, data describing turbidity at time-scales that may be important for primary productivity (e. g. days, hours) are not always available from field measurements. This study therefore developed a framework regarding the influence of turbidity on primary production and biomass around empirically measured levels of turbidity, including various theoretical ranges of variabilities around their means. In summary, production and biomass decreased with increasing turbidity and depth at St. Lucia, whereas the different levels of variability in turbidity were highly relevant to further our understanding of the impact of turbidity on microalgae production. A high variability in turbidity (i.e. an alteration of calm and windy days) reduced seasonal production at low mean turbidities and increased production at high mean turbidities in the model. Furthermore, a high variability of turbidity showed the potential to reduce or enhance the seasonal and annual pelagic and benthic production by more than 30% compared to that at low levels of variability. The day-to-day variability in turbidity therefore influences production in the long term. Another important point is that days with high and low mean turbidity do not necessarily counteract each other in terms of their effect on production, but that in addition to mean levels the extent of variability, preferably on a daily basis, should be taken into account when estimating primary production. Previous work highlights the importance of variable light conditions on primary production. For instance, the positive influence of variability in turbidity has been estimated to enhance primary production by 15% for the Neuse estuary in experiments using variable light conditions as opposed to static light conditions (Mallin and Paerl, 1992). Furthermore, Desmit et al. (2005) observed that even in high turbidity zones with high levels of variability of turbidity (Scheldt estuary, Belgium, The Netherlands), positive net phytoplankton production can be achieved. Conditions for bloom development can be dependent on the

variability of turbidity in addition to mean values as shown by a simulation study in South San Francisco Bay by May et al. (2003). Here, the variability of turbidity which was represented by diurnal wind conditions allowed for bloom development at similar wind speeds as during high wind speed scenarios when chl *a* concentrations remained low. The variability of turbidity and its consequences for microalgae production and biomass is of high importance for St. Lucia where water levels are highly variable and wind induced resuspension causes, at times, high levels of turbidity. Ranges of turbidities measured during the current study (1-915 NTU) coincide with those reported in the literature (2-1472 NTU by Cyrus, 1988, 0.7–1350 NTU by MacKay et al., 2010) and Cyrus (1988) attributed the high variability in turbidity to wind speed that varies on a daily and seasonal basis. The high turbidity values are facilitated in addition by the low water depths in Lake St. Lucia, when higher shear at the sediment surface facilitates higher rates of resuspension. Observations during the past 10 years show that water levels can vary to extreme extents. Whereas mean water depth in St. Lucia is about 1 m during times with an open mouth and average river run-off (Lawrie and Stretch, 2011), water depths as low as 0.1 m were observed in both North and South lake between 2004 and 2008, a period with below average rainfall (this study, MacKay et al., 2010). In individual years during the same period, even up to 90% of the lake area had been desiccated (e. g. in 2003, 2005 and 2006, Whitfield and Taylor, 2009), emphasising the high variability of water levels, and therefore turbidities. The effect of variability in water depths as opposed to static water levels was explored with the model. Its results suggest minor effects of seasonally varying water levels on annual microalgae production per area, and effects due to reduced habitat or increased salinities are likely to be of higher importance for microalgae and subsequently for higher trophic levels.

Due to the shallow water depths in Lake St. Lucia, light limitation was of minor importance in controlling primary production during the study period, despite of high turbidities. Instead, photoinhibition may have reduced primary production in the shallow water column on bright days. Microalgae production in turbid well mixed estuaries is generally thought to be unaffected by photoinhibition since the period that algal cells experience high light conditions in the surface layer is too short to induce photoinhibition (Grobbelaar, 1985). However, shallow depths allow for high irradiances (>600 μmol photons m^{-2} s^{-1}) in the entire water column, thus affecting algae sensitive to high light intensities. For example, MacIntyre and Cullen (1996) observed midday depression in primary production of the water column in the shallow San Antonio Bay (Texas, USA, 1–2 m deep) which they attributed to photoinhibition despite mainly turbid conditions (attenuations coefficients of 0.7–15 m^{-1}). Taking all of the above factors of water level, turbidity, light limitation, and photoinhibition into account, measured and simulated levels of turbidity and microalgae production and biomass fall within the range of previous empirical studies in Lake St. Lucia/other systems. Considering that St. Lucia constitutes 50% of the total estuarine area of South Africa and 80% of estuarine area in the province (approximately 500 km coastline), it is important to understand factors that influence the productivity of South Africa's largest nursery area.

4.1. Production under natural and managed conditions in Lake St. Lucia

We simulated primary production for different combinations of water depth and turbidity with a simplified model. Based on these model estimates and on area to depth relationships established by Hutchison (1976), we discuss the potential pelagic production for the entire lake system under different management scenarios. The St. Lucia lake system originally shared a common inlet with the Mfolozi river, which also provided the St. Lucia system with a significant freshwater supply (Lawrie and Stretch, 2011). Both systems were separated in the 1950s to prevent increasing silt loads reaching the lake system (Day et al., 1952; Taylor, 1982). The separation from the Mfolozi river affected the water level of Lake St. Lucia and resulted in very low water levels during years with below average rainfall (particularly in 2002–2011). Lawrie and Stretch (2011) estimated that the St. Lucia mouth would be closed for about 88% of the time in a system with separated inlets and water levels would be lower than the estuarine mean water level (corresponding to an average lake depth of ~1 m) for more than 40% of the time. In contrast, a combined inlet would lead to a predominantly open mouth (about 70% of the time) and water levels below the estuarine mean water level would occur for less than 6% of the time. Based on the probabilities for the occurrence of different water levels given by Lawrie and Stretch (2011) we estimated an average total production of 11.2 and $11.3 \cdot 10^3$ t C $year^{-1}$ for μ_{turb} = 40 NTU (σ_{turb} = 0.6) for separated and combined inlets, respectively. Production was similar when assuming higher turbidities at depths <0.5 m (μ_{turb} = 60, σ_{turb} = 0.6 for d < 0.5 and μ_{turb} = 40, σ_{turb} = 0.3 for $d \geq 0.5$) and was estimated as 11.4 and $12.5 \cdot 10^3$ t C $year^{-1}$, respectively. Between 2002 and 2011 extreme desiccation of Lake St. Lucia was observed (Whitfield and Taylor, 2009) reducing the lake area from ≈328 km^2 to <75 km^2 and consequently the mean lake depth. We estimated an annual pelagic primary production of $13.1 \cdot 10^3$ t C $year^{-1}$ for the 'full' system (0% desiccation) at a mean turbidity of 40 NTU. The model predicted similar or even higher total production, 14.8, 20.3 and $12.5 \cdot 10^3$ t C $year^{-1}$ for 25%, 50% and 75% desiccation, respectively. The same still holds when accounting for a potentially higher turbidity at low water depths (60 NTU for <0.5 m, 15.1, 20.4, 17.4 and $11.6 \cdot 10^3$ t C $year^{-1}$ for 0%, 25%, 50% and 75% desiccation, respectively). The high production in the desiccation scenarios in the model resulted from the lower mean depths of the lake (1.0, 0.7, 0.3 and 0.13 m for 0, 25, 50 and 75% desiccation, respectively, Hutchison, 1976.) which strongly enhanced light availability for microalgae and so consequently counteracted the effect of reduced lake area and volume. This means, microalgae potentially provided similar or even a higher production available for higher trophic levels under severe drought conditions when compared to wet conditions in Lake St. Lucia. The potentially higher microalgae production per area in extended shallow lake regions may not be utilised due to habitat loss for potential consumers or extreme hypersalinities as result of desiccation (Cyrus et al., 2011). Under hypersaline conditions when the water levels are lowest, most of the zoobenthos and zooplankton die off (Boltt, 1975; Jerling et al., 2010; Carrasco and Perissinotto, 2011). The loss of invertebrate food also places fish species under stress during such conditions, although some salt tolerant fish species can utilize alternative sources such as detritus and microalgae (Whitfield et al., 2006). Such extreme conditions with little grazing pressure by herbivores can promote algal blooms. For example, a cyanobacteria bloom developed in 2009 under hypersaline conditions (salinity regularly >100) in the northern lake basins and persisted with high biomasses for more than a year without being grazed (Muir and Perissinotto, 2011).

Altogether, our model provided a useful tool for the understanding of variable light availability for microalgae production in very shallow aquatic systems, and although inspired by observations from Lake St. Lucia, our results are more general and valid for similar systems. Therefore, our study serves as a framework for present and future studies on Lake St. Lucia. More comprehensive field measurements are necessary to understand the dynamics of the relationship between turbidity variability and food-web

dynamics, including information about resuspension of benthic microalgae and nutrients. Furthermore, the effects of variable salinity and temperature as well as wind driven horizontal mixing and dispersion are important particularly for understanding and predicting higher trophic levels.

Acknowledgements

We are very grateful to the management and staff of Ezemvelo KZN Wildlife and the iSimangaliso Wetlands Park, for providing logistical support during field studies. R. Taylor, C. Fox, and the late A. Myeza assisted with field operations. We thank R. Lawrie, C. Maine and J. Pringle for valuable discussions regarding water levels and turbidities, and R. Lawrie and J. Schoen for correcting the English. R. Perissinotto and all members and students of the Marine Biology group at SLS, UKZN are thanked for (assistance in) data collection. K.T. was funded by a post-doctoral scholarship from the School of Life Sciences at UKZN. Data acquisition was, for the most part, performed with support from the NRF (SEAChange, grant no 71051). We further appreciate support from SANPAD (grant no. 1090).

Appendix A

State variables and forcing data are named in upper case letters and are the following: B_{PA}, B_{BA} – biomass of pelagic and of benthic algae (mg C m^{-2}); N_{wc}, N_{pw} – nutrients in the water column and in the pore water (mg N m^{-2}); Q_{PA}, Q_{BA} – nutrient cell quota of pelagic and of benthic algae (–); G_{PA}, G_{BA} – density dependent mortality rate of pelagic and of benthic algae (day^{-1}); D – water depth (m), scenarios (i), (ii), (iii) (cf. Fig. 3; K_{sed} – light attenuation coefficient dependent on resuspended sediment (m^{-1}), derived from a linear model (cf. Section 2.1 Study site and field data, Fig. 2) with random turbidities from different distributions; *GlobI* – incident solar radiation (W m^{-2}), SASRI Weatherweb, conversion: 1 W m^{-2} = 4.6 μmol photons m^{-2} s^{-1}; T – water temperature (°C), derived from Eq. (A.37); S – salinity, dependent on water depth.

Processes and parameters are named in lower case letters, parameter values are given in Table 1. The following indices were used: *i*:*PA*,*BA*, referring to pelagic, and benthic algae fraction, respectively; *j*:*a*,*h*,*g*, referring to autotrophic, heterotrophic and grazing processes, respectively.

A.1. Equations to describe algae and nutrient dynamics

Pelagic and benthic algal biomass, B_i (mg C m^{-2}), i = *PA*,*BA*:

$$\frac{dB_i}{dt} = (r_i - a_i - b_i - m_i - G_i)\cdot B_i \tag{A.1}$$

Nutrient cell quota of algae, Q_i (–):

$$\frac{dQ_i}{dt} = v_i - r_i\cdot Q_i \tag{A.2}$$

Nutrient concentration in the water column, N_{wc} (mg N m^{-2}):

$$\frac{dN_{wc}}{dt} = +z\cdot eT_h\cdot\left(N_{tot} - N_{wc} - N_{pw} - \sum_i Q_i\cdot B_i\right) + \delta\cdot N_{pw} - v_{PA}\cdot B_{PA} - v_{BA\_wc}\cdot B_{BA} \tag{A.3}$$

Nutrient concentration in the pore water, N_{pw} (mg N m^{-2}):

$$\frac{dN_{pw}}{dt} = +z\cdot eT_h\cdot\left(N_{tot} - N_{wc} - N_{pw} - \sum_i Q_i\cdot B_i\right) - \delta\cdot N_{pw} - v_{BA\_pw}\cdot B_{BA} \tag{A.4}$$

A.2. Rate equations

Production rate (day^{-1}):

$$r_i^h\left(\text{hour}^{-1}\right) = r_i^0\cdot eI_i\cdot eQ_i\cdot T_a$$
$$r_i = \sum_h r_i^h \tag{A.5}$$

Respiration is separated into activity dependent respiration (Eq. (A.6)), which increases with increasing production, and basal respiration (Eq. (A.7)).

Activity dependent respiration rate (day^{-1}):

$$a_i = a^0\cdot r_i\cdot eS \tag{A.6}$$

Basal respiration rate (day^{-1}):

$$b_i = b^0\cdot eS\cdot eT_h \tag{A.7}$$

Mortality rate (day^{-1}):

$$m_i = m_i^0\cdot eS \tag{A.8}$$

Density dependent mortality rate (day^{-1}):

$$\frac{dG_i}{dt} = \frac{1}{\tau}\cdot\left(g_i^0\cdot B_i^{\alpha}\cdot\frac{eTg}{eS} - G_i\right) \tag{A.9}$$

Nutrient uptake rate of pelagic algae (mg N (mg C)$^{-1}$ day^{-1}):

$$v_{PA} = v_{PA}^0\cdot eT_a\cdot\frac{N_{wc\_vol}}{k_{PA} + N_{wc\_vol}}\cdot\left(1 - \frac{Q_{PA} - q_{min}}{q_{max} - q_{min}}\right) \tag{A.10}$$

Nutrient uptake rate of benthic algae (mg N (mg C)$^{-1}$ day^{-1}, assuming that both water column and pore water form independent nutrient sources):

$$v_{BA} = v_{BA\_wc} + v_{BA\_pw}$$
$$v_{BA\_wc} = v_{BA}^0\cdot eT_a\cdot\frac{N_{wc\_vol}}{k_{BA} + N_{wc\_vol}}\cdot\left(1 - \frac{Q_{BA} - q_{min}}{q_{max} - q_{min}}\right)$$
$$v_{BA\_pw} = v_{BA}^0\cdot eT_a\cdot\frac{N_{pw\_vol}}{k_{BA} + N_{pw\_vol}}\cdot\left(1 - \frac{Q_{BA} - q_{min}}{q_{max} - q_{min}}\right) \tag{A.11}$$

A.3. Equations of regulation factors

The variables *eI*, *eQ*, *eT*, and *eS* represent regulating factors that describe the response of primary production, nutrient uptake, respiration, mortality, and grazing mortality to light, nutrients, temperature, and salinity. As a general rule, the regulating factors are non-dimensional where a value of 1 represents optimal conditions, and values lower or larger than 1 represent suboptimal (i. e. limiting) conditions. As an exception, temperature regulation for respiration and remineralisation (eT_h, cf. Eq. (A.19)) is realised with a Q_{10} relationship where eT_h = 1 corresponds to reference conditions at a temperature of 20 °C and values lower or larger than 1 lead to lower or larger respiration or remineralisation rates, respectively.

eI_i — Light regulation factor, adopted from Baretta et al. (1995)

Light regulation factor of pelagic algae:

$$eI_{PA} = \frac{e^{\left(1-\frac{I_D}{I_{opt\_PA}}\right)} - e^{\left(1-\frac{I_0}{I_{opt\_PA}}\right)}}{\kappa_m \cdot D} \tag{A.12}$$

Light regulation factor of benthic algae:

$$eI_{BA} = \frac{I_D}{I_{opt\_BA}} \cdot e^{\left(1-\frac{I_D}{I_{opt\_BA}}\right)} \tag{A.13}$$

Light intensity at the surface of the water column:

$$I_0 = Globl^h \cdot q_{PAR} \tag{A.14}$$

Light intensity at the bottom of the water column:

$$I_D = I_0 \cdot e^{-\kappa \cdot D} \tag{A.15}$$

Light attenuation coefficient (m^{-1}):

$$\kappa = K_{sed} + \kappa_P \cdot B_{PA\_vol} \tag{A.16}$$

For derivation of eI_{PA} and eI_{BA} and description of I_{opt_PA} and I_{opt_BA} see Section A.4 Derivation of the light dependent production rate below. For $Globl^h$ see Section A.5 Calculation of irradiance per hour, Eq. (A.31).

eQ_i — Nutrient regulation factor (adopted from Wernicke and Nicklisch, 1986, Huber et al., 2008):

$$eQ_i = 1 - e^{\left(-ln2 \cdot \left(\frac{Q_i}{q_{min}} - 1\right)\right)} \tag{A.17}$$

eT_j — Temperature regulation factors (–):

Autotrophic processes (optimum curve, Arhonditsis and Brett, 2005):

$$eT_a = e^{\left(-h_{ta} \cdot (T - T_{opt})^2\right)} \tag{A.18}$$

Heterotrophic processes (Q_{10} relationship):

$$eT_h = Q_{10}^{\frac{(T-T_{ref})}{10}} \tag{A.19}$$

Density dependent mortality (optimum curve, Arhonditsis and Brett, 2005):

$$eT_g = e^{\left(-h_{tg} \cdot (T - T_{opt})^2\right)} \tag{A.20}$$

eS — Salinity regulation factor (adopted and adjusted from Griffin et al., 2001):

$$eS = \begin{cases} \frac{(\beta-1)}{S_{min}^2} \cdot S^2 - 2 \cdot \frac{(\beta-1)}{S_{min}} \cdot S + \beta, & \text{if } S < S_{min} \\ 1, \quad \text{if } S_{min} \le S \le S_{max} \\ \frac{(\beta-1)}{S_{max}^2} \cdot S^2 - 2 \cdot \frac{(\beta-1)}{S_{max}} \cdot S + \beta, & \text{if } S > S_{max}. \end{cases} \tag{A.21}$$

where $S_{min} \le S \le S_{max}$ represents the optimum salinity at which the value of $f(S)$ is 1.0. The relationship is parabolic, so that the effect of $f(S)$ is to increase the respiration rate or decrease the grazing rate as salinities reach values above or below the optimum salinity.

A.4. Derivation of the light-dependent production rate

The light-dependent production rate was estimated from a P–I curve following the formulation of Steele (1962) including photoinhibition at high light intensities:

$$p(I) = r \cdot \frac{I}{I_{opt}} \cdot e^{\left(1-\frac{I}{I_{opt}}\right)} \tag{A.22}$$

with r: potential growth rate, I_{opt}: optimum irradiance (cf. Eqs. (A.27), (A.30)).

Steele's model was used, because it allows for definition of a range of optimal light intensities. This means it allows for adaptation to changing irradiance based on e. g. adjustment of the photosynthetic apparatus, changes in species composition, or changes with seasons. The light intensity at which light dependent production becomes saturated (maximum) is described by the variables I_{opt_PA} and I_{opt_BA} in the model (Eqs. (A.27), (A.30)). This approach includes adaptation of algae to changing light intensities within a certain range of irradiances given by the parameters $I_{opt\_PA}^{min}$, $I_{opt\_PA}^{max}$, and $I_{opt\_BA}^{min}$ (Table 1). Different values of these parameters were tested in order to look at the effect of photoinhibition and the sensitivity of the model (see Appendix B).

A.4.1. Production of pelagic algae

Production of pelagic algae per hour ($prod_{PA}$) was averaged over the water column, and was calculated as:

$$prod_{PA} = \frac{1}{D} \int_0^D p_{PA}(I_z) dz \tag{A.23}$$

With

D:	total depth;
$p_{PA}(I_z)$:	production at depth z;
I_z:	photosynthetic active radiation at depth z; $I_z = I_0 \cdot e^{-\kappa \cdot z}$
I_0:	photosynthetic active radiation at the surface; $I_0 = q_{PAR} \cdot Globl^h$
q_{PAR}:	proportion of photosynthetic active radiation of global irradiance, q_{PAR}=0.45 (e. g. Kirk, 1994)
κ:	light attenuation coefficient (m^{-1}).

Substitution results in

$$prod_{PA} = \frac{1}{\kappa \cdot D} \int_{I_D}^{I_0} \frac{p_{PA}(I)}{I} dI \tag{A.24}$$

After substituting $p_{PA}(I)$ with Eq. (A.22), the resulting function of the primary production is:

$$prod_{PA} = \frac{1}{\kappa \cdot D} \cdot \int_{I_D}^{I_0} \frac{1}{I} \cdot r_{PA} \cdot \frac{I}{I_{opt\_PA}} \cdot e^{\left(1-\frac{I}{I_{opt\_PA}}\right)} dI \tag{A.25}$$

Integration results in:

$$prod_{PA} = r_{PA} \cdot \frac{1}{\kappa \cdot D} \cdot \left(e^{\left(1-\frac{I_D}{I_{opt\_PA}}\right)} - e^{\left(1-\frac{I_0}{I_{opt\_PA}}\right)}\right) \tag{A.26}$$

Optimum irradiance for pelagic algae (μmol photons m^{-2} s^{-1}):

$$I_{opt\_PA} = \begin{cases} I^{min}_{opt\_PA}, & \text{if } I_m < I^{min}_{opt\_PA} \\ I_m, & \text{if } I^{min}_{opt\_PA} < I_m < I^{max}_{opt\_PA} \\ I^{max}_{opt\_PA}, & \text{if } I_m > I^{max}_{opt\_PA} \end{cases} \quad (A.27)$$

with $I^{max}_{opt\_PA} = 600$ and $I^{min}_{opt\_PA} = 150$ μmol photons m^{-2} s^{-1}

The range of saturating light intensities is highly species specific. We here chose general values for algal communities (Lampert and Sommer, 1997; Reynolds, 2006) and tested lower and higher values in the sensitivity analysis.

Radiation integrated over the water column (μmol photons m^{-2} s^{-1}):

$$I_m = I_0 \cdot \frac{\left(1 - e^{(-\kappa \cdot D)}\right)}{\kappa \cdot D} \quad (A.28)$$

A.4.2. Production of benthic algae

Production of benthic microalgae ($prod_{BA}$) per hour was calculated directly from Eq. (A.22) with $I = I_D$ and $I_{opt} = I_{opt\_BA}$ (Eq. (A.29)). It was assumed that benthic algae experience the light intensity that reaches the bottom of the water column (I_D), their onset of saturating light intensity is lower than that of pelagic algae, and production is not reduced at high irradiances due to photoinhibition (Barranguet et al., 1998; Dodds et al., 1999).

$$prod_{BA} = r_{BA} \cdot \frac{I_D}{I_{opt\_BA}} \cdot e^{\left(1 - \frac{I_D}{I_{opt\_BA}}\right)} \quad (A.29)$$

Optimum irradiance for benthic algae (μmol photons m^{-2} s^{-1}):

$$I_{opt\_BA} = \begin{cases} I^{min}_{opt\_BA}, & \text{if } I_D < I^{min}_{opt\_BA} \\ I_D, & \text{if } I_D > I^{min}_{opt\_BA} \end{cases} \quad (A.30)$$

with $I^{min}_{opt\_BA} = 50$ μmol photons m^{-2} s^{-1}

A.5. Calculation of irradiance per hour

Irradiance per hour (adopted from Ebenhöh, 1997; Kohlmeier, 2004):

$$GlobI^h = \max\left[0, \frac{GlobI}{q_p} \cdot \left(\cos\left(\frac{t_r}{2 \cdot q_p}\right) + \cos^2\left(\frac{t_r}{2 \cdot q_p}\right)\right)\right] \quad (A.31)$$

with t_r= daytime in rad $[-\pi,\pi]$: $t_r = 2 \cdot \pi \cdot t_h - 12/24$ (t_h= daytime in h [0,24]) and q_p= fraction of the day the sun is up (Eq. (A.32)).

Fraction of the day the sun is up (adopted from H. Glarner, http://www.gandraxa.com/length_of_day.xml):

$$q_p = \begin{cases} 0, & \text{if } \frac{\arccos(1-M)}{\pi} < 0 \\ \frac{\arccos(1-M)}{\pi}, & \text{if } 0 \le \frac{\arccos(1-M)}{\pi} \le 1 \\ 1, & \text{if } \frac{\arccos(1-M)}{\pi} > 1 \end{cases} \quad (A.32)$$

$$M = 1 - \tan(Lat) \cdot \tan(Axis \cdot \cos(J \cdot Day)) \quad (A.33)$$

with $Lat = -28 \cdot \pi/180$ rad, $Axis = 23.439 \cdot \pi/180$ rad, $J = \pi/182.625$ rad, and Day= day of year [0.365]

A.6. Conversion of values per area in values per volume

$$B_{PA\_vol} = \frac{B_{PA}}{D} \quad (A.34)$$

$$N_{wc\_vol} = \frac{N_{wc}}{D} \quad (A.35)$$

$$N_{pw\_vol} = \frac{N_{pw}}{0.01} \quad (A.36)$$

only the upper centimetre of the sediment was accounted for processes important for primary production

A.7. Temperature time series (adopted from Kohlmeier, 2004)

$$T = T_{mean} - T_a \cdot \cos\left(2 \cdot \pi \cdot \frac{Day - d_{min}}{y}\right) \quad (A.37)$$

with $T_{mean} = 22$ °C (mean annual temperature), $T_a = 6$ (variability in temperature), $d_{min} = 196$ doy (coldest day of the year), $y = 365.25$ days (length of year), Day= day of year [0, 365]

Appendix B

B.1. Effects of photoinhibition

To investigate the effect of different optimum light parameters for the P–I curve as well as the effect of photoinhibition we run simulations without photoinhibiton and with changed I_{opt} parameters. We tested the effect of photoinhibition by comparing the net primary production of the standard scenario ($150 \le I_{opt\_PA} \le 600$ μmol photons m^{-2} s^{-1}) with a scenario without photoinhibition ($I_{opt\_PA} \ge 150$ μmol photons m^{-2} s^{-1}). Furthermore, we ran a scenario with saturating light intensities shifted to a lower range ($75 \le I_{opt\_PA} \le 300$ μmol photons m^{-2} s^{-1} i. e. stronger photoinhibition, but less light limitation compared to the standard scenario) and compared the results with the scenario without photoinhibition. We calculated the percentage change in seasonal production from the scenario without photoinhibition (x_1 in Eq. (3) main text) to the scenarios with photoinhibition (x_2 in Eq. (3) main text) and its error (Eq. (4) main text).

Photoinhibition reduced seasonal production by up to 16% and the seasonal standing stock by up to 10% at low turbidities (<20 NTU) or at low water depth (0.2 m) with the parameters used in our model (Fig. B.1 A). Increasing turbidity diminished the effect of photoinhibition. Shifting the range of saturating light intensities to lower irradiance values, $75 \le I_{opt\_PA} \le 300$, led to the onset of photoinhibition at lower light intensities (>300 μmol photons m^{-2} s^{-1}). At the same time, light limitation at low light intensities was reduced. Comparison with the model run with $I_{opt\_PA} \ge 150$ μmol photons m^{-2} s^{-1} showed a strong effect of photoinhibition at low water depth and low turbidity, where seasonal production was reduced by ~50% (Fig. B.1 B). In contrast, at high turbidity in deeper water (e. g. 0.8 m and 200 NTU, Fig. B.1 B), seasonal production was enhanced by up to ~40% as a result of the reduced light limitation, but this was only valid for less variable turbidities.

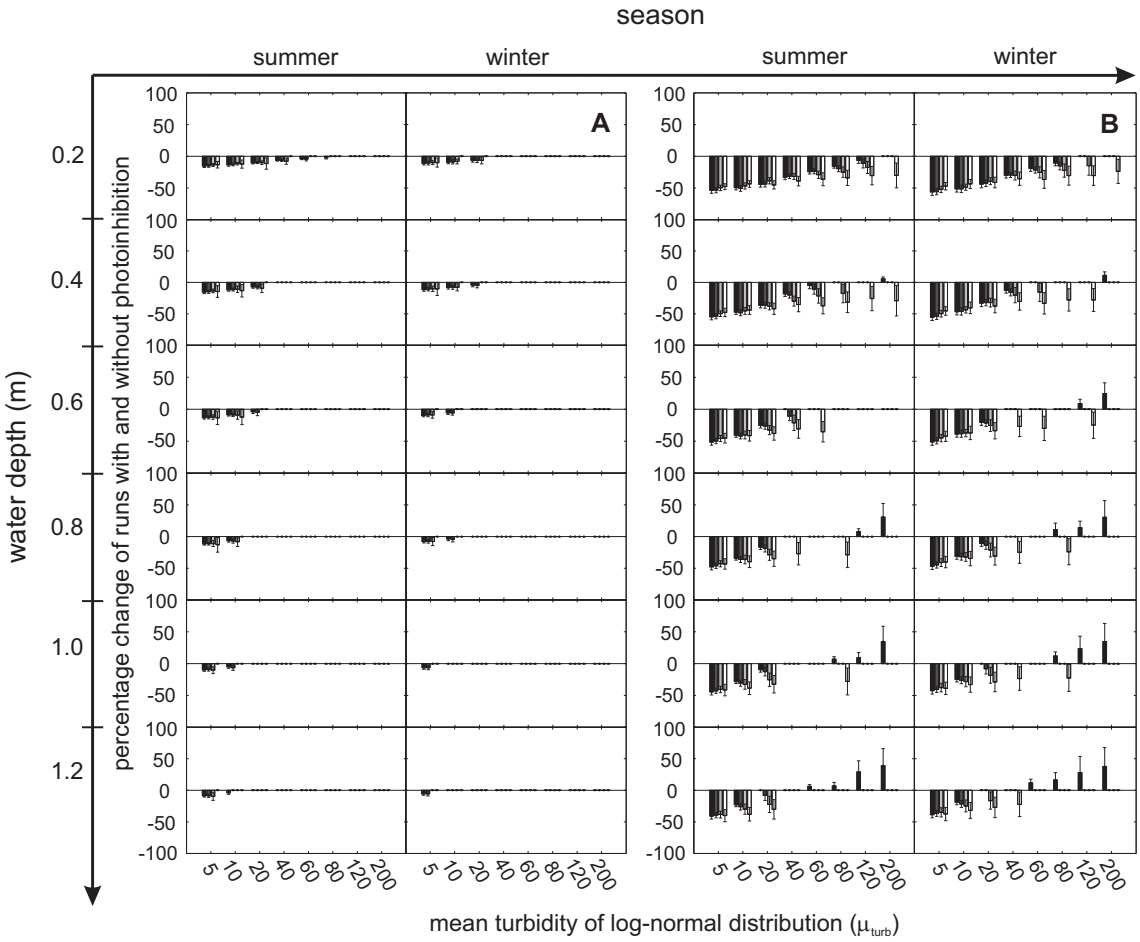

Figure B.1. Percentage change in net primary production of pelagic algae of (A) a run without photoinhibition, I_{opt_PA}>150 μmol photons m^{-2} s^{-1}, and the standard run with photoinhibition, 150<I_{opt_PA}<600 μmol photons m^{-2} s^{-1}, and (B) a run without photoinhibition and a run with the saturating light intensities shifted to a lower range, 75<I_{opt_PA}<300 μmol photons m^{-2} s^{-1} (i. e. stronger photoinhibition, but less light limitation) in summer and winter for different mean turbidities (x-axis) and different water depth (panels from top to bottom). Bars as in Fig. 5.

B.2. Sensitivity analysis

We tested the sensitivity of the result variables seasonal net primary production, average biomass, balance of pelagic versus benthic production, and average P:B ratio (production to biomass) to changes in different model parameters. We ran simulations with altered parameter values for three water depths (0.2, 0.6, and 1.0 m), three values of μ_{turb} (10, 40, 80 NTU), and two values of σ_{turb} (0.15, 0.6) representing lower, medium, and higher values of the appropriate variable. We then calculated the standardised sensitivity of model results as:

$$\frac{\Delta var}{\Delta par}\cdot\frac{par_{standard}}{var_{standard}} \qquad \text{(B.1)}$$

We used a basic local sensitivity analysis where only one parameter is changed at a time and all others are kept at their "standard" values (see Table 1 in main text). The aim here was to determine to what extend the model is influenced by the parameters defining light adaptation compared to growth/grazing parameters. Thus, we altered $I^{opt}_{min\_i}$ and $I^{opt}_{max\_PA}$ by ±50%, and the potential growth rate (r_i) and the density dependent grazing parameter (g_i) by ±25%. In addition, we tested a lower total nutrient concentration (N_{tot} −50%) and a 10 times higher diffusion rate of pore water nutrients into the water column (δ•10). Such a high diffusion rate could represent resuspension of nutrients, which was otherwise not included. Altering total nutrient concentration, the diffusion of nutrients from pore water and the parameters of the P–I curves of pelagic and benthic algae had only minor effects on the overall model results (Fig. B.2). A higher sensitivity of model results was observed with changes in the growth rates and grazing rates. The model was most sensitive to changes in the growth rate of benthic algae (Fig. B.2). Decreasing the total nutrient concentration resulted in reduced net primary production and biomass of both pelagic and benthic algae. A 10-fold higher diffusion rate of nutrients from the pore water into the water column did not change the overall pattern for the different depths and turbidities, but it increased the production at high depth and high turbidity. Changes in the P–I curves had the expected effects on pelagic and benthic algae; an enlarged range of saturating light intensities (reduced I^{min}_{opt} or increased I^{max}_{opt}) resulted in higher net production, biomass, and P:B. A reduced range of saturating light intensities (increased I^{min}_{opt} or decreased I^{max}_{opt}) resulted in lower net production, biomass, and P:B. The algae fraction whose parameters remained unchanged, was hardly affected. The majority of the values of sensitivity to the I_{opt} parameters lay within ±0.5, indicating that a change in the parameters by 50% resulted in a change in the result variables by less than 25%. Altering the growth rates of pelagic and benthic algae had large effects on net production and biomass on occasion, in particular for benthic microalgae. This was also reflected in the sensitivity of the balance between pelagic and benthic gross production, whereas the ratio of production to biomass (P:B) was much less affected. The sensitivity analysis showed that the model is much more sensitive to uncertainties in the growth and grazing

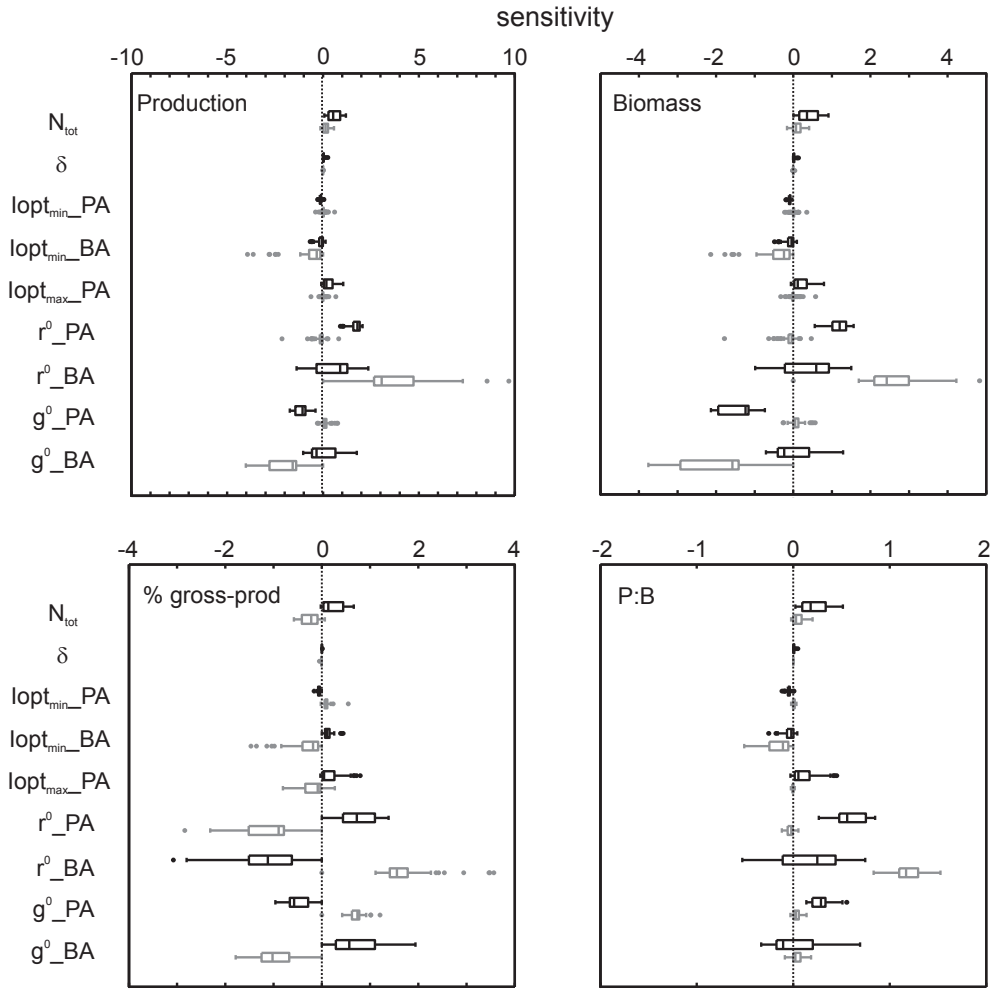

Figure B.2. Sensitivity of model results (net production, biomass, balance of pelagic and benthic production as percentage of total gross production, P:B ratio) to different parameters. Sensitivity was calculated as the ratio of percentage change of the model results and parameter (Eq. (B.1)). Positive values indicate that an increase (decrease) in a parameter value caused an increase (decrease) of the result variable and negative values indicate the opposite effect on the result variable. Note the different scales. Boxplots include sensitivity calculated for increased and decreased parameters for the 2 seasons, different depths, different mean turbidities, and different standard deviations (cf. B.2 Sensitivity analysis), i. e. a total of 72 values (outliers outside 1.5 interquartile range). Black boxes – pelagic algae, grey boxes – benthic algae. x-scales were reduced for visibility, few outliers lay outside the shown range: 1 outlier for benthic net production, 4 outliers for benthic algal biomass, 2 outliers for benthic percentage of total gross production.

parameters than to uncertainties in the P–I curves, which means that the questions tested with this model here would be affected only to a comparatively small extent by more specific P–I curves.

References

Adams, J., Bate, G., 1999. Primary producers, estuarine microalgae. In: Allanson, B.R., Baird, D. (Eds.), Estuaries of South Africa. Camebridge University Press, pp. 91–100.

Anandraj, A., Perissinotto, R., Nozais, C., Stretch, D., 2008. The recovery of microalgal production and biomass in a South African temporarily open/closed estuary, following mouth breaching. Estuar. Coast. Shelf Sci. 79, 599–606 http://dx.doi.org/10.1016/j.ecss.2008.05.015. http://linkinghub.elsevier.com/retrieve/pii/S0272771408002230.

Arhonditsis, G.B., Brett, M.T., 2005. Eutrophication model for Lake Washington (USA) Part I. Model description and sensitivity analysis. Ecol. Model. 187, 140–178 http://dx.doi.org/10.1016/j.ecolmodel.2005.01.040.

Baretta, J., Ebenhöh, W., Ruardij, P., 1995. The European regional seas ecosystem model, a complex marine ecosystem model. Neth. J. Sea Res. 33, 233–246 http://dx.doi.org/10.1016/0077-7579(95)90047-0.

Barranguet, C., Kromkamp, J., Peene, J., 1998. Factors controlling primary production and photosynthetic characteristics of intertidal microphytobenthos. Mar. Ecol. Prog. Ser. 173, 117–126 http://dx.doi.org/10.3354/meps173117.

Blasutto, O., Cibic, T., Vittor, C.D., Umani, S.F., 2005. Microphytobenthic primary production and sedimentary carbohydrates along salinity gradients in the lagoons of grado and marano (northern adriatic sea). Hydrobiologia 550, 47–55.

Boltt, R.R., 1975. The benthos of some southern African lakes. Part 5: the recovery of the benthic fauna of St Lucia following a period of excessively high salinity. Trans. Royal Soc. S. Afr. 41, 295–323.

Canion, A., Macintyre, H.L., Phipps, S., 2013. Short-term to seasonal variability in factors driving primary productivity in a shallow estuary: Implications for modeling production. Estuar. Coast. Shelf Sci. 131, 224–234 http://dx.doi.org/10.1016/j.ecss.2013.07.009. http://dx.doi.org/10.1016/j.ecss.2013.07.009.

Carrasco, N.K., Perissinotto, R., 2010. In situ feeding rates and grazing impact of *Mesopodopsis africana* O. Tattersall in the St Lucia Estuary, South Africa. J. Exp. Mar. Biol. Ecol. 396, 61–68 http://dx.doi.org/10.1016/j.jembe.2010.09.008. http://linkinghub.elsevier.com/retrieve/pii/S0022098110003862.

Carrasco, N.K., Perissinotto, R., 2011. Temperature and salinity tolerance of *Mesopodopsis africana* O. Tattersall in the freshwater-deprived St. Lucia Estuary, South Africa. J. Exp. Mar. Biol. Ecol. 399, 93–100 http://dx.doi.org/10.1016/j.jembe.2011.01.014. http://linkinghub.elsevier.com/retrieve/pii/S002209811100027X.

Cloern, J., 1987. Turbidity as a control on phytoplankton biomass and productivity in estuaries. Cont. Shelf Res. 7, 1367–1381 http://dx.doi.org/10.1016/0278-4343(87)90042-2.

Cloern, J.E., Foster, S.Q., Kleckner, A.E., 2013. Review: phytoplankton primary production in the world's estuarine-coastal ecosystems. Biogeosci. Discuss. 10, 17725–17783.

Cyrus, D., 1988. Turbidity and other physical factors in Natal estuarine systems part 1: selected estuaries. J. Limnol. Soc. South. Afr. 14, 60–71.

Cyrus, D., Jerling, H., MacKay, F., Vivier, L., 2011. Lake St Lucia, Africa's largest estuarine lake in crisis: combined effects of mouth closure, low levels and hypersalinity. South Afr. J. Sci. 107, 1–13 http://dx.doi.org/10.4102/sajs.v107i3/4.291.

Cyrus, D., Vivier, L., Jerling, H., 2010. Effect of hypersaline and low lake conditions on ecological functioning of St Lucia estuarine system, South Africa: an overview 2002–2008. Estuar. Coast. Shelf Sci. 86, 535–542 http://dx.doi.org/10.1016/j.ecss.2009.11.015. http://linkinghub.elsevier.com/retrieve/pii/S0272771409005307.
Cyrus, D.P., 1989. The Lake St Lucia system – a research assessment. South Afr. J. Aquatic Sci. 15, 3–25.
Day, J.H., Millard, N.A.H., Broekjuysen, G.J., 1952. The ecology of South African estuaries. Part IV: the St. Lucia system. Trans. Royal Soc. S. Afr. 34, 129–156.
Desmit, X., Vanderborght, J., Regnier, P., Wollast, R., 2005. Control of phytoplankton production by physical forcing in a strongly tidal, well-mixed estuary. Biogeosciences 2, 205–218.
Dodds, W.K., Biggs, B.J.F., Lowe, R.L., 1999. Photosynthesis-irradiance patterns in benthic microalgae: variations as a function of assemblage thickness and community structure. J. Phycol. 35, 42–53 http://dx.doi.org/10.1046/j.1529-8817.1999.3510042.x.
Droop, M.R., 1983. 25 years of algal growth kinetics – a personal view. Bot. Mar. 26, 99–112.
Dyer, K.R., 2000. Estuaries: a Physical Introduction. John Wiley & Sons, New York.
Ebenhöh, W., 1997. The primary production module in the marine ecosystem model ERSEM II, with emphasis on the light forcing. J. Sea Res. 38, 173–193 http://dx.doi.org/10.1016/S1385-1101(97)00043-9.
Fielding, P., Forbes, A., Demetriades, N., 1991. Chlorophyll concentrations and suspended particulate loads in St Lucia, a turbid estuary on the east coast of South Africa. South Afr. J. Mar. Sci. 11, 491–498.
Geider, R., 1992. Respiration: taxation without representation? In: Falkowski, P., Woodhead, A. (Eds.), Primary Productivity and Biogeochemical Cycles in the Sea. Plenum Press, New York, pp. 333–360.
Griffin, S.L., Herzfeld, M., Hamilton, D.P., 2001. Modelling the impact of zooplankton grazing on phytoplankton biomass during a dinoflagellate bloom in the Swan River Estuary, Western Australia. Ecol. Eng. 16, 373–394 http://dx.doi.org/10.1016/S0925-8574(00)00122-1.
Grobbelaar, J.U., 1985. Phytoplankton productivity in turbid waters. J. Plankton Res. 7, 653–663.
Huber, V., Adrian, R., Gerten, D., 2008. Phytoplankton response to climate warming modified by trophic state. Limnol. Oceanogr. 53, 1–13.
Hutchison, I.P.G. (Ed.), 1976. The Hydrology of the St Lucia System. 1976 Proc: St Lucia Scientific Advisory Council Workshop: Charter's Creek: Feb 1976.
Jassby, A.D., Cloern, J.E., Cole, B.E., 2002. Annual primary production: patterns and mechanisms of change in a nutrient-rich tidal ecosystem. Limnol. Oceanogr. 47, 698–712 http://dx.doi.org/10.4319/lo.2002.47.3.0698. http://www.aslo.org/lo/toc/vol_47/issue_3/0698.html.
Jerling, H.L., Vivier, L., Cyrus, D.P., 2010. Response of the mesozooplankton community of the St Lucia estuary, South Africa, to a mouth-opening event during an extended drought. Estuar. Coast. Shelf Sci. 86, 543–552 http://dx.doi.org/10.1016/j.ecss.2009.11.014.
Johnson, I.M., 1977. A Study of the Phytoplankton of the St Lucia Systems. Master's thesis. Botany Department, University of Natal.
Kirk, J.T., 1994. Light and Photosynthesis in Aquatic Ecosystems. Camebridge University Press.
Kohlmeier, C., 2004. Modellierung des Spiekerooger Rueckseitenwatts mit einem gekoppelten Euler-Lagrange-Modell auf der Basis von ERSEM. Ph.D. thesis. Carl von Ossietzky Universitaet Oldenburg.
Krause-Jensen, D., Sand-Jensen, K., 1998. Light attenuation and photosynthesis of aquatic plant communities. Limnol. Oceanogr. 43, 396–407.
Lake, S.J., Brush, M.J., 2011. The contribution of microphytobenthos to total productivity in upper Narragansett bay, Rhode Island. Estuar. Coast. Shelf Sci. 95, 289–297.
Lampert, W., Sommer, U., 1997. Limnoecology. Oxford University Press.
Lawrie, R.A., Stretch, D.D., 2011. Anthropogenic impacts on the water and salt budgets of St Lucia estuarine lake in South Africa. Estuar. Coast. Shelf Sci. 93, 58–67 http://dx.doi.org/10.1016/j.ecss.2011.04.005.
MacIntyre, H., Cullen, J., 1996. Primary production by suspended and benthic microalgae in a turbid estuary: time-scales of variability in San Antonio Bay, Texas. Mar. Ecol. Prog. Ser. 145, 245–268 http://dx.doi.org/10.3354/meps145245.
MacKay, F., Cyrus, D., Russell, K.-L., 2010. Macrobenthic invertebrate responses to prolonged drought in South Africa's largest estuarine lake complex. Estuar. Coast. Shelf Sci. 86, 553–567 http://dx.doi.org/10.1016/j.ecss.2009.11.011.
Mallin, M.A., Paerl, H.W., 1992. Effects of variable irradiance on phytoplankton productivity in shallow estuaries. Limnol. Oceanogr. 37, 54–62.
May, C., Koseff, J., Lucas, L., Cloern, J., Schoellhamer, D., 2003. Effects of spatial and temporal variability of turbidity on phytoplankton blooms. Mar. Ecol. Prog. Ser. 254, 111–128.
McLusky, D., Elliott, M., 2004. The Estuarine Ecosystem: Ecology, Threats and Management. Oxford University Press, Oxford.
Miller, D.C., Geider, R.J., MacIntyre, H.L., 1996. Microphytobenthos: the ecological role of the "secret garden" of unvegetated, shallow-water marine habitats. II. Role in sediment stability and shallow-water food webs. Estuaries 19, 202–212. http://dx.doi.org/10.2307/1352225. http://www.springerlink.com/index/10.2307/1352225.
Mitbavkar, S., Anil, A., 2004. Vertical migratory rhythms of benthic diatoms in a tropical intertidal sand flat: influence of irradiance and tides. Mar. Biol. 145, 9–20.
Van der Molen, J.S., Perissinotto, R., 2011. Microalgal productivity in an estuarine lake during a drought cycle: the St. Lucia Estuary, South Africa. Estuar. Coast. Shelf Sci. 92, 1–9 http://dx.doi.org/10.1016/j.ecss.2010.12.002.
Montes-Hugo, M., Alvarez-Borrego, S., Gaxiola-Castro, G., 2004. Annual phytoplankton production in a coastal lagoon of the southern California current system. Mar. Ecol. Prog. Ser. 277, 51–60.
Muir, D.G., Perissinotto, R., 2011. Persistent phytoplankton bloom in Lake St. Lucia (iSimangaliso Wetland Park, South Africa) caused by a cyanobacterium closely associated with the genus Cyanothece (synechococcaceae, chroococcales). Appl. Environ. Microbiol. 77, 5888–5896 http://dx.doi.org/10.1128/AEM.00460-11.
Nche-Fambo, F.A., 2014. The Dynamics of Nano- and Microplankton in the St. Lucia Estuarine Lake System, KwaZulu-natal. Master's thesis. University of KwaZulu-Natal.
Nel, H., 2011. Salinity tolerance of the bivalve Solen cylindraceus (Hanley, 1843) (Mollusca: Euheterodonta: Solenidae) in the St Lucia estuary. Afr. Invertebr. 52, 575–586.
Perissinotto, R., Bate, G., Muir, D.G., 2013. Microalgae. In: Perissinotto, R., Stretch, D.D., Taylor, R.H. (Eds.), Ecology and Conservation of Estuarine Ecosystems: Lake St. Lucia as a Global Model. Cambridge University Press, pp. 187–208.
Perissinotto, R., Pillay, D., Bate, G., 2010. Microalgal biomass in the St Lucia Estuary during the 2004 to 2007 drought period. Mar. Ecol. Prog. Ser. 405, 147–161 http://dx.doi.org/10.3354/meps08542.
Pillay, D., Perissinotto, R., 2008. The benthic macrofauna of the St. Lucia estuary during the 2005 drought year. Estuar. Coast. Shelf Sci. 77, 35–46 http://dx.doi.org/10.1016/j.ecss.2007.09.004.
Pillay, D., Perissinotto, R., 2009. Community structure of epibenthic meiofauna in the St. Lucia estuarine lake (South Africa) during a drought phase. Estuar. Coast. Shelf Sci. 81, 94–104.
Potter, I.C., Chuwen, B.M., Hoeksema, S.D., Elliott, M., 2010. The concept of an estuary: a definition that incorporates systems which can become closed to the ocean and hypersaline. Estuar. Coast. Shelf Sci. 87, 497–500 http://dx.doi.org/10.1016/j.ecss.2010.01.021. http://linkinghub.elsevier.com/retrieve/pii/S0272771410000363.
Pringle, J., 2011. Wind Induced Sediment Re-suspension in a Shallow Lake. Master's thesis. University of KwaZulu-Natal.
Reynolds, C., 2006. Ecology of Phytoplankton. Camebridge University Press.
Scheffer, M., 1998. Ecology of Shallow Lakes. Kluwer Academic Publishers.
Sommer, U., 1991. A comparison of the droop and the Monod models of nutrient limited growth applied to natural populations of phytoplankton. Funct. Ecol. 5, 535–544 http://dx.doi.org/10.2307/2389636.
Steele, J., 1962. Environmental control of photosynthesis in the sea. Limnol. Oceanogr. 7, 137–150.
Taylor, R.H. (Ed.), 1982. St. Lucia Estuary: the Aquatic Environment – the Physical and Chemical Characteristics. St Lucia Research Review Natal Parks Game and Fish Preservation Board, Queen Elizabeth Park, Pietermaritzburg.
Taylor, R.H., 2006. Ecological Responses to Changes in the Physical Environment of the St Lucia Estuary. Ph.D. thesis. Norwegian University of Life Sciences, Department of Plant and Environmental Sciences.
Tirok, K., Gaedke, U., 2007. The effect of irradiance, vertical mixing and temperature on spring phytoplankton dynamics under climate change: long-term observations and model analysis. Oecologia 150, 625–642. http://dx.doi.org/10.1007/s00442-006-0547-4.
Underwood, G., Kromkamp, J., 1999. Primary production by phytoplankton and microphytobenthos in estuaries. Adv. Ecol. Res. 26, 93–153.
Wernicke, P., Nicklisch, A., 1986. Light/dark cycle and temperature — their impact on phosphate-limited growth of *Oscillatoria redekei* VANGOOR in semi-continuous culture. Int. Rev. Gesamten Hydrobiol. 71, 297–313.
Whitfield, A.K., 1992. A characterization of Southern African estuarine systems. South Afr. J. Aquatic Sci. 1, 89–103.
Whitfield, A.K., Taylor, R.H., 2009. Case studies and reviews A review of the importance of freshwater inflow to the future conservation of Lake St Lucia. Aquatic Conserv.: Mar. Freshw. Ecosyst. 19, 838–848 http://dx.doi.org/10.1002/aqc.
Whitfield, A.K., Taylor, R.H., Fox, C., Cyrus, D.P., 2006. Fishes and salinities in the St Lucia estuarine system a review. Rev. Fish. Biol. Fish. 16, 1–20 http://dx.doi.org/10.1007/s11160-006-0003-x.
Winter, D., 1999. Chemistry, biochemical processes. In: Allanson, B.R., Baird, D. (Eds.), Estuaries of South Africa. Camebridge University Press, pp. 70–76.